INSTITUTE OF PHYSICS PUBLISHING MEASUREMENT SCIENCE AND TECHNOLOGY

Meas. Sci. Technol. **16** (2005) R65–R92 doi:10.1088/0957-0233/16/6/R01

REVIEW ARTICLE

AFM: a versatile tool in biophysics

Andrea Alessandrini and Paolo Facci

INFM National Research Center on 'nanoStructures and bioSystems at Surfaces-S3', Via Campi 213/A, 41100 Modena, Italy

E-mail: p.facci@unimo.it

Received 10 September 2004, in final form 2 March 2005
Published 28 April 2005
Online at stacks.iop.org/MST/16/R65

Abstract

Here we review the applications of atomic force microscopy to the study of samples of biological origin. Emphasis is given to provide the reader with information on the broad range of different biophysical applications that, to date, such a technique can deal with. After recalling briefly the operating principles of an atomic force microscope, the broad field of bio-imaging applications is faced (DNA, DNA–protein interaction, proteins, lipid membranes, cells); thereafter, the use of the atomic force microscope to measure forces is introduced and force mapping on living cells is discussed. This section is followed by the description of the use of force curves in assessing single-molecule inter- and intramolecular interactions. A paragraph on the perspectives of the technique in biophysical applications concludes the paper. We hope that this review can help the reader in appreciating how atomic force microscopy contributes to the current explosive growth of nanobiosciences, where biology, chemistry and physics merge.

Keywords: AFM, biophysics, force spectroscopy, DNA, DNA–protein interaction, proteins, lipids, membranes, cells

(Some figures in this article are in colour only in the electronic version)

1. Introduction

The atomic force microscope (AFM) [1] belongs to the broad family of scanning probe microscopes in which a proximal probe is exploited for investigating properties of surfaces with subnanometre resolution. The AFM, initially developed to overcome the limitations of its ancestor, the scanning tunnelling microscope (STM) [2], in imaging non-conducting samples, immediately attracted the attention of the biophysical community [3–10]. At the beginning the emphasis was mainly on the improved imaging resolution compared to that of optical microscopy, but, soon after, it became clear that AFM was much more than just a high-resolution microscope. The possibilities of spectroscopic analysis, surface modification and molecular manipulation gave rise to a real breakthrough in the realm of AFM use.

In biological applications, the most appealing advantage of the AFM as a high-resolution microscope in comparison with other techniques such as SEM and TEM, is that it allows measurements of native biological samples in physiological-like conditions [11, 12], avoiding complex sample preparation procedures and artefacts connected to them. The use of mild imaging conditions opened the way to dynamic studies in which conformational changes and molecular interactions could be followed in real time at single-molecule level. The set of samples of biological interest studied by AFM ranges nowadays from the smallest biomolecules, such as phospholipids, proteins, DNA, RNA, to subcellular structures (e.g. membranes), all the way down to living cells and tissues. Not only structural properties can be investigated, but also mechanical or chemical and functional properties are the focus of many AFM applications. In this review we will outline the application of the AFM in the biophysical science. We will start with a brief description of how the AFM works, then we will review the applications of the technique as far as imaging is concerned, starting from DNA and proteins to living cells; afterwards we will move to non-imaging techniques in which the method of force curves is exploited to investigate molecular

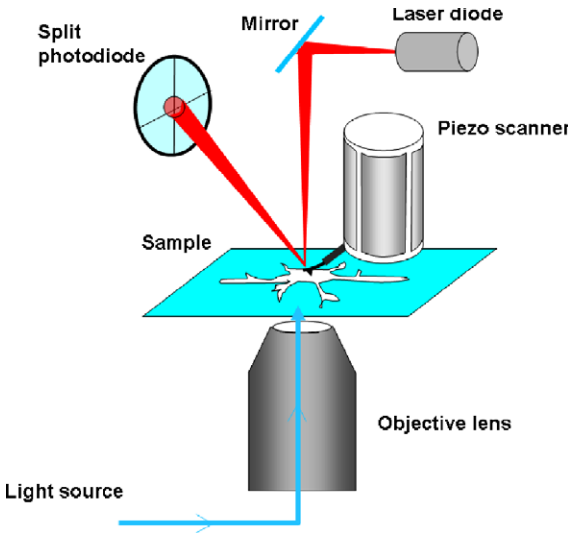

Figure 1. Scheme of an AFM coupled with an inverted optical microscope.

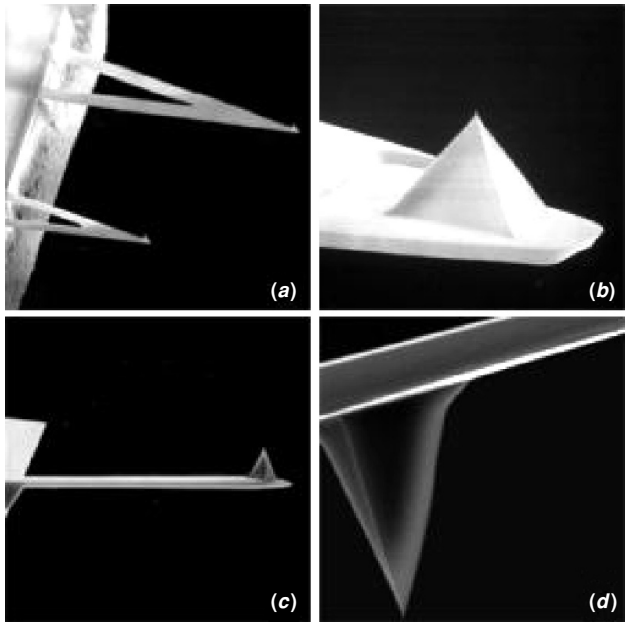

Figure 2. Scanning electron microscope images of microfabricated AFM cantilevers and tips. (*a*) Silicon nitride cantilevers and (*b*) high magnification of the tip with oxide-sharpened apex; (*c*) silicon cantilever and (*d*) high magnification of the silicon tip. Courtesy of Veeco Instruments.

interactions. At the end we will summarize the possible future trends in this field enumerating the most promising forthcoming technical developments and appealing scientific problems that could be faced using the AFM.

2. Fundamental elements of the atomic force microscope

Several excellent reviews can be found in the literature on issues related to instrumental aspects of the AFM [13–15] and we direct the reader to them for a more exhaustive review. In what follows we will just briefly recall the operating principles of an AFM and will summarize the imaging modes that are of main interest to biophysical research.

2.1. How does the AFM work?

The AFM works by scanning, in a raster fashion, a very tiny tip mounted at the end of a flexible microcantilever in gentle touch with the sample. This relative motion is performed with sub-Angstrom accuracy by a piezoelectric actuator (usually a tube, sometimes a tripod). Interacting with the sample the cantilever deflects and the tip–sample interaction can be monitored with high resolution exploiting a laser beam impinging on the back of the cantilever [16]. The beam is reflected towards a split photodetector configuring an optical lever which amplifies cantilever deflections. In almost all operating modes, a feedback circuit, connected to the cantilever deflection sensor, keeps tip–sample interaction at a fixed value controlling the tip–sample distance. The amount of feedback signal, measured at each scanning point of a 2D matrix, concurs to form a 3D reconstruction of the sample topography which is usually displayed as an image. In figure 1 a scheme of an AFM is reported in a typical configuration for biological applications, where it is coupled with an optical microscope to simultaneously acquire an optical image and the surface topography with the AFM.

2.2. Cantilevers and tips

The scanning probe is the heart of the AFM, as for every scanning probe-based technique. The most common cantilevers used nowadays are realized by exploiting silicon micromachining technology [17–19]. In figure 2(*a*) a scanning electron microscope image of a silicon nitride microfabricated cantilever chip, usually used for contact AFM, is shown. At the end of a cantilever a tiny pyramid, the tip, is integrated (figure 2(*b*)). Depending on the imaging mode adopted, different types of cantilevers and tips may be used. When the AFM is operated in the static contact mode, the stiffness of the cantilever should be as low as possible (less than the interatomic spring constant of atoms in a solid), whereas in dynamic operation modes (see below) higher values for the spring constant help us reduce noise and instabilities. Figure 2(*c*) reports an image of a silicon cantilever and tip, usually used in dynamic operation modes, and a magnified view of the integrated silicon tip is shown in figure 2(*d*). Typical spring constants for AFM cantilevers range from 0.01 N m^{-1} to 100 N m^{-1}, enabling a force sensitivity down to 10^{-11} N. The limit in force sensitivity is related to an interplay between thermal, electrical and optical noise.

The use of carbon nanotubes as AFM tips, figure 3, has represented a great breakthrough in terms of resolution [20–23]. Carbon nanotube tips possess a high aspect ratio, mechanical robustness, small diameter and a well-defined surface chemistry. They can be chemically functionalized, and appear to be the ideal probe for biological applications of the AFM requiring high resolution, particularly in the case of structural biology. The high-resolution imaging capabilities of carbon nanotube tips have been demonstrated on a variety of biological samples, such as DNA, IgG, IgM, GroES, SWI/SNF. The resolution attainable with carbon nanotube

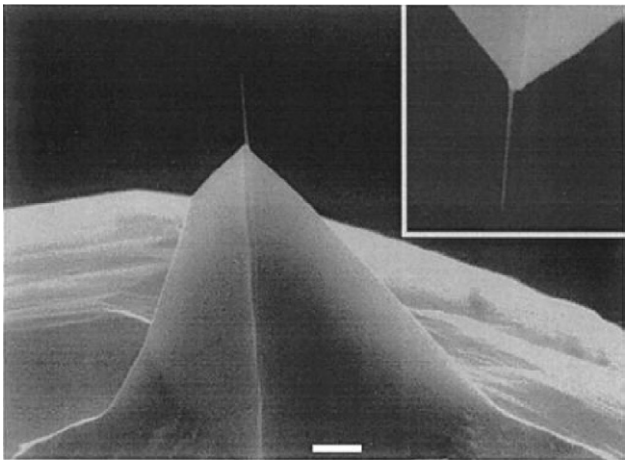

Figure 3. Multiwall carbon nanotube tip attached to the end of single-crystal silicon tip. The inset is a higher magnification view of the same tip rotated 180° relative to the main image (bar = 1 μm). Reprinted with permission from [22]. Copyright 1998, American Chemical Society.

tips is comparable with that of other ultimate resolution imaging techniques such as cryogenic electron microscopy, but carbon nanotubes offer also the possibility to be functionalized, exposing, thus, a well-defined chemical group or chemisorbed biomolecule. This opportunity can be exploited to study the spatial distribution of chemical functional groups or complementary biomolecules in a sample.

2.3. Imaging modes

The classification of the possible operation modes is strictly related to the region of the force field between the tip and the sample spanned by the tip during imaging. Considering a non-linear force field composed of a repulsive short range force (<1 nm) and an attractive long range one (van der Waals force, <100 nm), depending on the force experienced by the tip–cantilever ensemble, three working methods for the atomic force microscope can be defined. If the force between the tip and the sample is always repulsive and the tip is constantly in contact with the sample the microscope works in the contact mode. If the tip experiences only an attractive force with the sample and it never touches the sample, the usually called true-non-contact mode is being used. If the tip experiences both the attractive and the repulsive force with the sample, the intermittent-contact mode is used. In the following we will describe AFM imaging modes of interest for biological application. It is to be stressed that here only modes pertaining to imaging will be discussed, while other applications of the AFM, more closely related to force spectroscopy, will be discussed in a separate section.

The first imaging mode which has been developed is the contact mode, in which the tip is constantly in gentle touch with the sample surface [1]. In this imaging mode the applied force, hence cantilever deflection, is kept constant by the feedback system while the tip scans the surface. Images are created by recording the piezo-vertical position required to keep the force constant. This mode of operation can be used under aqueous environments allowing a reduction of the interaction force between the tip and the sample with respect to operation in air. The interaction force reduction comes

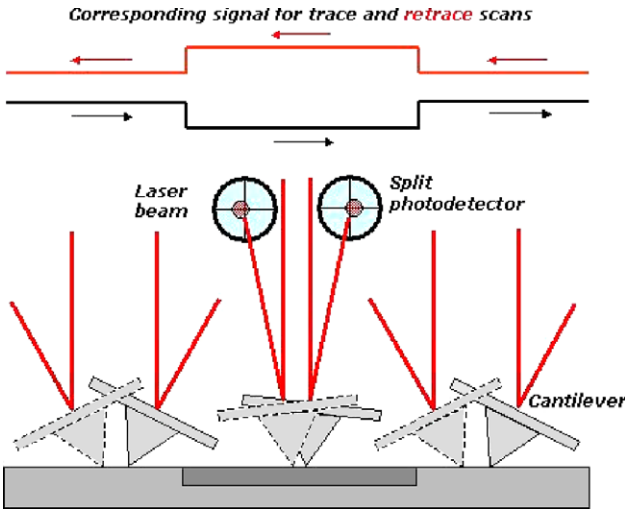

Figure 4. Operating principle of the lateral force mode. The signal from the lateral segments of the photodetector is monitored while the tip is scanned on the surface in the direction perpendicular to the major axis of the cantilever. Both the trace and retrace signals are recorded to avoid possible interference of the topographic signal with the lateral force signal. Indeed, a pure lateral force should give an inverted signal in the trace and retrace scan of the tip. Subtracting the two signals (trace and retrace) highlights the contrast coming only from lateral forces.

from the removal of capillary forces due to the presence of a thin water layer on surfaces in air [24]. This mode is the one of choice as far as flat and rather rigid samples are involved (e.g. reconstituted membranes, 2D protein crystals) enabling the highest resolution level. Sometimes, image artefacts, such as tilt of the surface or drift of the scanner perpendicular to the surface, dominate the topography image over real topographical features, especially when imaging is performed over large areas with slow scan rate. To avoid low-frequency artefacts the error mode can be used [25], in which the cantilever deflection signal is recorded keeping the feedback response time as fast as possible. The error signal gives a measure of how well the feedback system is maintaining the desired deflection setpoint. Due to the finite response time of the feedback loop, high-frequency signals cannot be completely compensated, and the cantilever will not be always at the same deflection value, especially in the case of high-frequency signals, generating a compensation error, which can be exploited to obtain an image rich in information. Moreover, tilt and vertical drift of the scanner generally have a low frequency and do not contribute to the error-mode image.

When the tip is scanned in contact with the sample, lateral forces arise which cause a torsion of the cantilever. The torsion can be monitored by the signal from lateral segments of the photodiode [26]. Recording the torsion of the cantilever, surface distribution of different chemical functionalities, which result in different friction or adhesion properties with the tip, can be mapped. This operation mode is usually referred to as lateral force mode or, when chemically modified tips are used to measure differences between areas of distinct chemical properties, the technique is referred to as 'chemical force microscopy' [27]. Figure 4 shows a scheme of this operation mode.

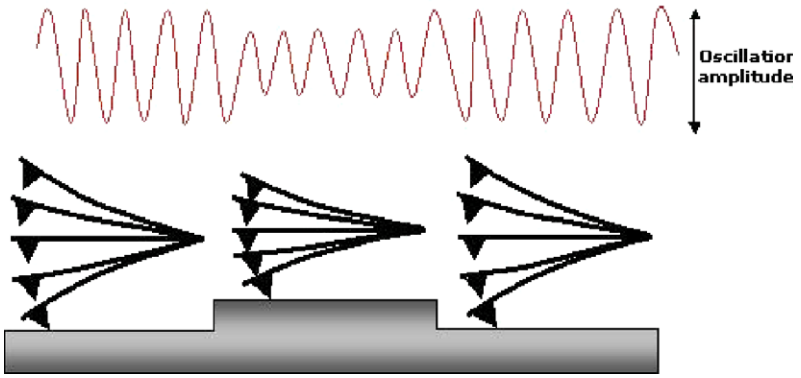

Figure 5. Schematic representation of an AFM tip operating in the intermittent contact mode.

A drawback of the contact mode is the development of dragging forces associated with the lateral movement of the tip in contact with the sample. This problem is particularly evident in the case of biological samples, which are usually loosely bound to the substrate and easily damageable.

To overcome this problem another mode of operation, the intermittent contact mode, has been developed (figure 5) [28]. In this case the cantilever is oscillated at a frequency near its resonance and the oscillation amplitude is monitored. Starting from a free oscillation amplitude, when the cantilever approaches the sample and starts to hit its surface, the oscillation amplitude is damped. By recording the feedback signal required to keep the amplitude constant, the topography of the sample surface can be obtained. The tip being only intermittently in contact with the sample, the dragging forces during scanning are greatly reduced [29]. In the intermittent contact mode the tip goes through both the attractive and the repulsive regions of the tip–sample force field during oscillation. The operation setpoint can be chosen so as to make attractive forces the dominant ones reducing damage to the sample and sometimes increasing resolution [30].

Technically, the cantilever can be oscillated by two methods [31]: acoustically or magnetically. In the first case the cantilever is oscillated by a piezo-actuator in contact with the cantilever supporting chip, whereas in the second case the cantilever is oscillated by means of an alternating magnetic field which acts on a magnetically susceptible film deposited on the backside of the cantilever [32]. Furthermore, important information on the viscoelastic properties of the sample can be retrieved by monitoring the phase difference between the cantilever driving signal and the output oscillation signal [33]. In particular, the phase shift is strictly related to the amount of energy dissipated in the tip–sample contact and a mapping of the phase shift on a sample surface allows us to identify regions of different interaction properties [34, 35]. The development of intermittent contact modes of operation in liquid configured an important breakthrough for the application of the AFM in biology, especially in the case where single loosely immobilized molecules have to be imaged [36, 37]. Imaging at high resolution (about 1 nm) by intermittent contact mode AFM in liquid on biological samples has been reported [38], allowing us also to retrieve information about the interaction forces from the phase signal [39].

Dealing with the intermittent contact mode in liquid, a new technique which has been recently introduced for controlling in a better way the force applied by the tip is active quality factor control (active-Q) [40, 41]. This is a technique which allows us to increase the otherwise low quality factor for the oscillating cantilever in liquid and correspondingly to decrease the force applied by the tip on the sample.

2.4. Some considerations about resolution

Apical curvature radii of commercially available tips can be as small as 2 nm. However, spatial resolution is not simply related to this aspect; rather, it depends also on the type of sample being imaged. At variance with the scanning tunnelling microscope, in the AFM the interaction developing between probe and sample is not limited to the two nearest atoms of the tip and sample; long-range forces can also play a significant role, involving a huge number of atoms contributing to the contrast formation mechanism. Even if true atomic resolution images have been obtained by the AFM on layered samples [42], this resolution level is only possible in particular cases. As a general rule, the harder and flatter the sample the higher the spatial resolution achievable. Often, the resolution obtained is higher than that expected on the basis of the nominal value of the apical curvature radius, due to the presence of nanoasperities which may play the role of the true imaging tip [43]. The dependence of AFM resolution on the softness of the sample is of remarkable importance especially for biological samples, usually very soft and damageable during scans. Spatial resolution down to subnanometre level on biological samples has been obtained in the case of proteins in reconstituted membranes, which show a closely packed 2D molecular array; however, in the case of isolated proteins the resolution drops to a few nanometres. The resolution attainable is even worse, being in the range of a few tens of nanometres, in the case of living cells, due to the softness of the cell membrane. Moreover, the surface chemistry of the tips, usually not well defined, may limit the application of AFM in the investigation of biological samples. However, resolution is not only a question of tip dimensions. For example, the accurate control of the interaction between the tip and sample in dynamic operation modes, balancing the contribution of attractive and repulsive forces, can greatly enhance resolution [30].

3. Bio-imaging applications

3.1. DNA and DNA–protein interaction

Since the advent of atomic force microscopy, DNA has been the most studied sample among those of biological origin. DNA is now considered as the reference bio-sample against which new technical developments are tested [44]. The number of AFM experiments involving DNA further increased as a consequence of the development of the intermittent contact mode imaging technique in liquid [36, 37] which allowed the imaging of DNA molecules loosely bound to the substrate without problems connected to the dragging forces arising in contact mode experiments. This technique also allowed, as we will see below, the possibility of studying DNA–protein interaction in physiological conditions. So far, only rarely has image resolution reached the level needed to resolve the major groove of dsDNA [45], but improvements in the technique, especially regarding the tip, are expected to provide significant advancements in resolution. The first critical aspect to be taken into account for imaging DNA by AFM is its immobilization on a solid substrate. As a general consideration, AFM is a technique which probes a surface and biophysicists have to develop suitable strategies for immobilizing their samples at surfaces [46]. Ideally, the best immobilization approach should provide bonds between the molecule and surface strong enough to avoid the dragging effects induced by the scanning tip. However, the sample should still have enough mobility as to retain its native structure and, possibly, functionality. In the case of DNA the substrate of choice is mica, a mineral belonging to the silicate class, which provides an atomically flat surface with negative surface charge (arising from the surface exposed OH moieties) upon cleaving and immersion in aqueous solution. DNA immobilization is usually achieved by introducing divalent cations in solution which act as bridges between the negatively charged mica surface and the negatively charged DNA phosphate backbone [47–49]. Other surfaces used for immobilizing DNA include 3-aminopropyltriethoxysilane functionalized mica [50] or mica coated with Langmuir–Blodgett films [51]. Besides, the effect of substrate and sample preparation methods on the imaged conformation of the DNA has been investigated [52, 53]. In particular, the effect of the transition from three to two dimensions on DNA conformation and the consequent re-equilibration of the polymer on the surface have been elucidated. Once DNA arrives on the surface from solution it has two possibilities: (1) it can undergo relaxation at the surface reaching its equilibrium conformation; (2) it can adhere on the surface without equilibration, resembling a sort of projection of the 3D conformation on the surface (trapping condition). Which of the two situations takes place is a question pertaining to sample deposition protocol [54] and the nature of the surface onto which it is deposited [55]. The end-to-end distance of small DNA fragments on the substrate is a parameter which is usually exploited to determine if DNA deposition has been carried out under equilibrium conditions [54].

AFM images of DNA usually report a width of the molecule which is larger than the known diameter of the molecule (∼2 nm, from x-ray diffraction data) [56, 57]. This is a typical feature of AFM measurements which arises when the radius of curvature of the tip is comparable with the dimensions of the imaged sample. The resulting image is a convolution of tip and sample geometry which leads to a widening of the sample structure. Using carbon nanotube tips, an apparent diameter of about 4.3 nm has been obtained [58]. However, in the case of DNA the apparent width also depends on the imaging conditions, including adhesion and humidity effects when it is imaged in air, and on the kind of solvent used during imaging [59] under liquid. Also the applied force influences DNA width as measured by AFM [59]. The measured height of DNA is another intriguing aspect of AFM imaging. Usually, it results to be less than the expected figure. The presence of a salt adlayer coating the substrate uniformly and acting as a height reference background may be the reason for this underestimate, but also the deformation of DNA under applied force should be considered [60]. It should be stressed that even if forces may be in the pico-newton range, the pressure applied can still be very high due to the small contact area.

The supercoiling of DNA molecules has been the subject of several studies, exploiting the topographic information given by AFM, which represent an advantage over electron microscopy [61]. Another advantage of AFM over electron microscopy is that ionic concentration is well defined when imaging is performed in liquid, whereas it becomes completely undefined when the sample is dried [62]. Also in this case, it is important to make use of trapping conditions which guarantee that DNA can preserve its native conformation once on the surface. When supercoiled DNA molecules are adsorbed on freshly cleaved mica, images show molecules in the shape of an open circle, evidencing relaxation on the surface. If the same molecules are deposited on spermine- or spermidine-treated mica, supercoiling is retained confirming that a trapping condition has been established which prevents DNA equilibration [53]. The height information has also been exploited to study the sequence-specific binding of particles or enzymes, such as the formation of 20 nucleotide triple helices [63] and G-wire quadruple helices in the presence of specific metal cations [64]. Other AFM investigations on DNA include the analysis of the radiation damage on DNA structure [65–68] and the structural perturbation induced by intercalating agent [69, 70]. The effect of ethidium bromide on the tertiary structure of DNA has been observed both in air [71] and in real time in liquid [62]. In both cases, an increase in ethidium bromide concentration leads to the formation of regions of plectonemic supercoiling.

Also DNA–protein interactions have been the object of several studies, performed both on dried samples and under physiological-like environment. DNA conformation near the protein binding site has been studied, including looping [72, 73], bending [74–76] and supercoiling [77]. When working in a physiological environment, biochemical processes have been followed in real time. For these studies the development of the intermittent contact mode in liquid has been critical, because it has allowed high-resolution imaging along with reduced dragging forces. Using this mode, immobilization of molecules on the surface can be so loose to enable their relative motion, guaranteeing, at the same time, high-resolution imaging. The random walk of *Escherichia coli* RNA polymerase (RNAP) along the DNA chain has been imaged in the case of non-specific complexes [78]. Figure 6

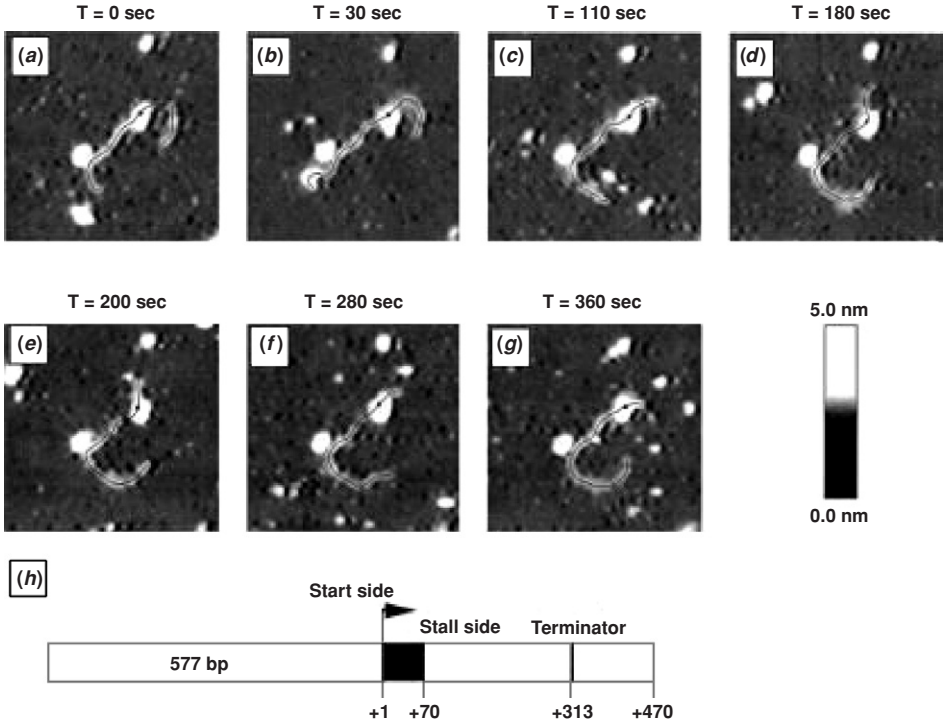

Figure 6. Tapping mode images showing the dynamics of a transcribing RNAP. (*a*) Image of the complex before the injection of NTP into the liquid cell. (*b*)–(*g*) Time-lapse images after transcription was resumed by injecting NTP into the imaging solution. In (*h*) the map of the DNA template used in the experiment is reported, with the sequence allowing the formation of the stalled elongation complex (1–70) highlighted. Reprinted with permission from [78]. Copyright 1999, Biophysical Society.

shows the dynamics of a transcribing RNAP. Upon addition of nucleoside triphosphates to the sample cell, the transcription was resumed, with the RNAP stably bound to the mica surface and the DNA sliding through the protein.

Other DNA–protein interactions studied by AFM include the tumour suppressor p53 protein bound to supercoiled and linear DNA [79, 80] and the CBF3–centromere DNA complexes [81]. DNA condensates have attracted a large number of AFM investigations, regarding also the dynamics of DNA condensation [82]. Different shapes of polycation-induced condensates such as flowerlike structures or toroids of different size, have been imaged. It has been shown that DNA condensation may be induced on the surface by silanes or protoamines, forming even larger condensates with respect to solution.

The study of chromatin by AFM represents a great challenge, its structure and molecular determinants not yet being fully understood [83–85]. AFM has allowed the elucidation of the correlation between the number of nucleosomes and the shortening of the DNA. Wang *et al* [86] managed to immobilize chromatin on glutaraldehyde (GD) modified mica allowing at the same time high-resolution imaging and the possibility of inducing structural modifications upon changes in environmental conditions, e.g. salt concentration (figure 7). Using this surface, the histonic proteins are covalently linked to GD-mica, while DNA is not constrained to the surface. By this approach, in a salt titration experiment, the complete loss of DNA from the polynucleosomal array at higher salt concentration has been real time followed *in situ*.

3.2. Proteins

Immediately after its invention, the potentialities of AFM for studying proteins were demonstrated [87, 88]. Both soluble and membrane proteins have been studied, revealing submolecular details. Developments both in sample preparation [46, 89] and in imaging condition/techniques [21, 43] allowed us to achieve images with resolution in the subnanometre range. In the case of isolated proteins, the resolution obtained is lower with respect to membrane proteins which can form closely packed 2D crystalline layers. It has been shown that imaging conditions, such as pH and salt concentration, may play an important role and are usually different for the immobilization and imaging steps of biological samples. A proper environment ensures imaging with forces in the order of some tens of pico-newtons, preventing sample distortion or disruption. Moreover, varying the imaging force, it is possible to shed light onto induced structural changes, using the AFM as a nanotool to manipulate single molecules [90]. In the following we will review AFM imaging of the two classes of water-soluble and membrane proteins.

The isolated components of the GroES chaperone machinery have been imaged in contact mode down to a lateral resolution of 1–2 nm [91]. The individual subunits of the GroES heptamer were clearly resolved together with the central depression. In this case, this level of resolution was reached only upon glutaraldheyde sample fixation. The use of carbon nanotube tips allowed a great improvement in resolution enabling the possibility of revealing submolecular details without sample fixation (figure 8) [92]. Isolated

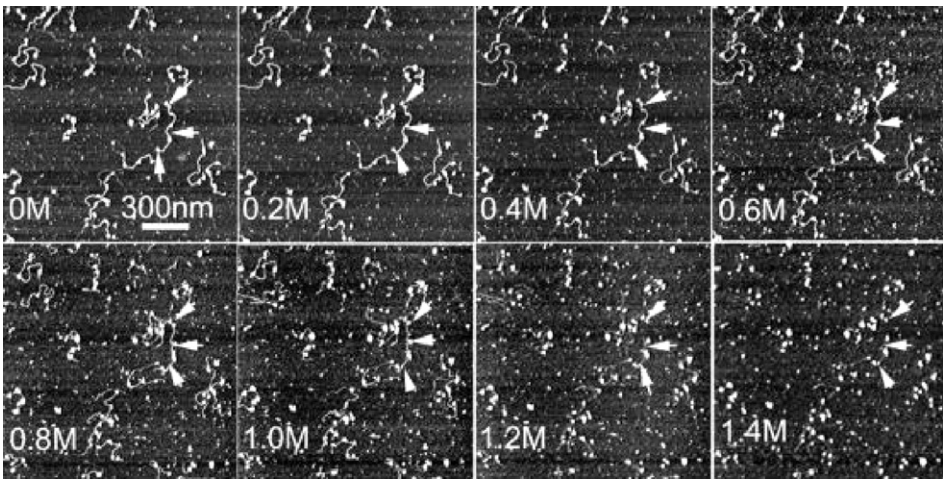

Figure 7. Series of images taken over the same region of the deposited sample as the salt concentration is increased in steps from 0 to 1.4 M. The vertical scale (black to white) is 3 nm. The sample is a reconstituted MMTV polynucleosomal promoter array (the same molecule is identified by arrows in each image). The DNA is completely lost from the array by 1.2 M NaCl. Note how the histone protein remains fixed in place on the substrate, whereas the DNA is free to move. Reprinted with permission from [86]. Copyright 2002, Biophysical Society.

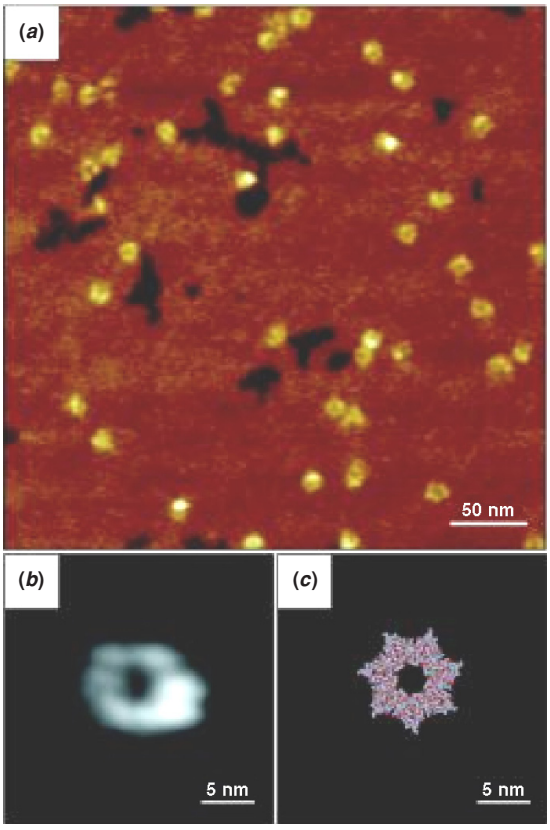

Figure 8. GroES imaged by a CVD-grown nanotube tip. The large scan area in (*a*) shows both 'dome' and 'pore' conformations, representing the two sides of GroES facing up. (*b*) A higher resolution image of the pore side shows the heptameric symmetry, which matches well with the crystal structure (*c*). Reproduced with permission from [92]. Copyright 2000, National Academy of Sciences, USA.

IgG and IgM antibody proteins have been imaged by AFM, revealing, when imaged at cryogenic temperatures, the typical Y-shape [93]. Even in this case carbon nanotube tips allowed

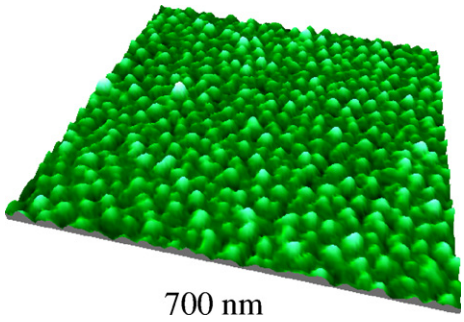

Figure 9. Magnetic alternating contact mode topography image of a submonolayer of the blue copper protein azurin chemisorbed on mica derivatized by 3-mercaptopropyltrimethoxysilane. Azurin chemisorption takes place via the competition of the free thiol of the silane with the intramolecular SS bond of the protein (Cys3Cys26).

resolution of the Y-shape IgG structure at room temperature and of the pentameric structure of IgM antibodies, revealing also the loop structure connecting two of the five Fc domains (joining loop) [92, 94].

In the majority of the cases, when isolated water-soluble proteins have to be imaged by AFM, they are immobilized on a substrate exploiting a suitable chemistry in order to sustain the scanning force of the tip. Using naturally occurring or protein engineering introduced functional surface groups it is possible to covalently bind proteins to a substrate enabling AFM to provide an estimate of the quality of the molecular layer which may be of interest for bioelectronics or biosensor applications (figure 9) [95, 96].

When membrane proteins packed into 2D crystalline arrays are imaged by AFM, subnanometre-scale lateral resolution images may be obtained. The high signal-to-noise ratio of AFM images enables us to retrieve structural details of biological molecules at the single-molecule level, making this technique the only one capable of imaging samples at this resolution level in physiological environment. X-ray diffraction and cryo-transmission electron microscopy (TEM) are the most frequently used techniques for obtaining structural

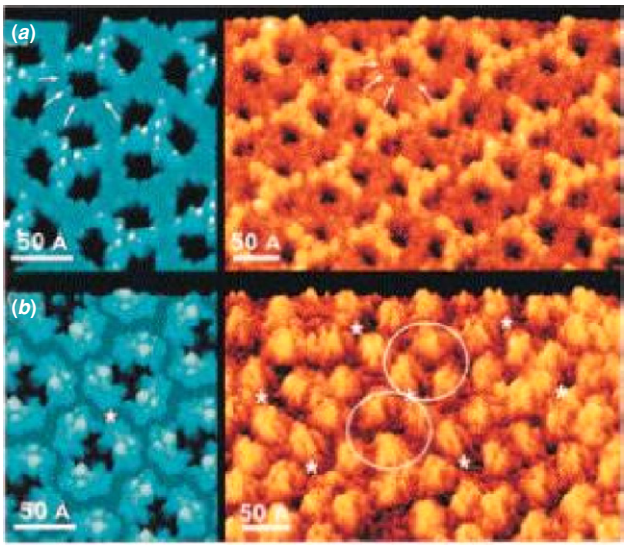

Figure 10. Conformational changes of porin OmpF. (*a*) The atomic model of the periplasmic surface rendered at 0.3 nm resolution (left) exhibits features which are recognized in the topograph (right). (*b*) The extracellular surface of OmpF. Atomic model (left), and topograph (right). Reprinted with permission from [97]. Copyright 1999, Elsevier Science.

details of transmembrane proteins. Comparisons between high-resolution topography images of membrane proteins acquired by AFM and atomic models derived from x-ray crystallography correlate very well. Figure 10 shows an example of this correlation in the case of the porin outer membrane protein F (OmpF) [97] imaged in a liquid environment at minimal tip–sample interaction force. This protein assumes a stable trimeric structure in the outer membrane of *E. coli* and is responsible for the passage of solutes across the membrane. In figure 10(*a*), the periplasmic surface (atomic model on the left, AFM image on the right) of a porin OmpF crystal reconstituted in the presence of dimyristoyl phosphatidylcholine is shown, whereas figure 10(*b*) shows the extracellular surface. The extracellular surface was exposed by exploiting the AFM tip to remove the first layer of the double layer structure in which the proteins assemble forming the crystal [98]. A deviation from the atomic model, which represents an average result, may be ascribed to long and flexible loops protruding from the membrane. Indeed, comparing average and standard deviation maps it is also possible to distinguish between common structural details of the proteins and regions characterized by structural variability. Other membrane proteins which have been imaged at subnanometre resolution are the light-driven proton pump bacteriorhodopsin that is regularly packed in the purple membrane of *Halobacterium salinarum* [99]; the hexagonally packed intermediate (HPI) layer from *Deinococcus radiodurans* [100]; molecular motors such as F_0F_1-adenosine triphosphate (ATP) synthase [101] and the ϕ 29 rotary motor [102] identifying in both cases the subunits constituting the proteins; bacterial water channels such as Aquaporin 1 [103], Aquaporin Z [104] and the Aquaporin 0 (or major intrinsic protein, MPI) [105]. As a general rule, AFM does not have a resolution as high as that provided by x-ray or electron crystallography, but its main advantages lie in the real space imaging and in the possibility of monitoring conformational changes of proteins *in situ*. However, all the mapped structural changes were done on protein with known structures that had been solved using traditional methods. On completely unknown structures the AFM image interpretation would be of huge difficulty.

Among the conformational changes studied by AFM, the channel closure of OmpF porins induced by voltage drop, pH and K^+ gradient variations is of particular relevance [97]. The extracellular polypeptides loops are flexible domains which have been shown to collapse towards the trimer centre formed by individual porin in response to an electric potential >200 mV across the membrane (in this case the membrane is deposited on conductive highly oriented pyrolitic graphite, HOPG), a K^+ gradient > 0.3 M and a pH < 3. The conformational changes of the cytoplasmic and extracellular surface of gap junction plaques have been visualized by AFM in buffer solution [106]. In particular, the extracellular conformational changes in the presence of Ca^{2+}, namely the reduction of the channel entrance diameter, were identified. Also the membrane protein diffusion in the lipid membrane has been followed in the case of sodium-driven rotors ATP synthase from *Ilyobacter tartaricus* by repeated imaging of the same area (figure 11) [107]. It is to be stressed that the movement of individual proteins was not influenced by the scanning direction of the tip. The diffusion coefficient obtained by AFM images was lower than what was expected for the diffusion of membrane protein in a free-standing membrane. The lower diffusion coefficient may be related to the fact that the membrane is supported by mica to allow high-resolution imaging.

AFM is also employed in the study of membrane proteins in native membrane patches even if at lower resolution. Membrane patches from *Xenopus laevis* oocytes are usually used, because it is quite easy to heterologously express the proteins of interest. Different methods have been developed to image by AFM both the extra- and intra-side of the plasma membrane deposited on a solid support [108]. Also nuclear pores in the nuclear membranes isolated from *Xenopus* oocytes have been imaged in near physiological conditions, following conformational changes in real time in response to ATP, calcium and pH [109]. Routine identification by AFM of a specific membrane protein embedded in native membranes is a difficult task; towards this goal the membrane can be incubated with antibodies, possibly conjugated to gold colloids [110], against the protein of interest which can be clearly identified by the height increment in the surface topography due to the bound antibody.

3.3. Supported lipid films

AFM is a powerful technique also for studying supported lipid films [111, 112]. Its potentialities come from the capacity of imaging lipid films at high lateral and vertical resolution in a liquid environment, the ability of investigating local mechanical properties and interaction force and the possibility of using the AFM tip as a nanotool to locally modify the films. Samples are usually prepared by using a Langmuir–Blodgett trough which allows us to transfer lipid films from the air–water interface to a solid support. Both monolayers and

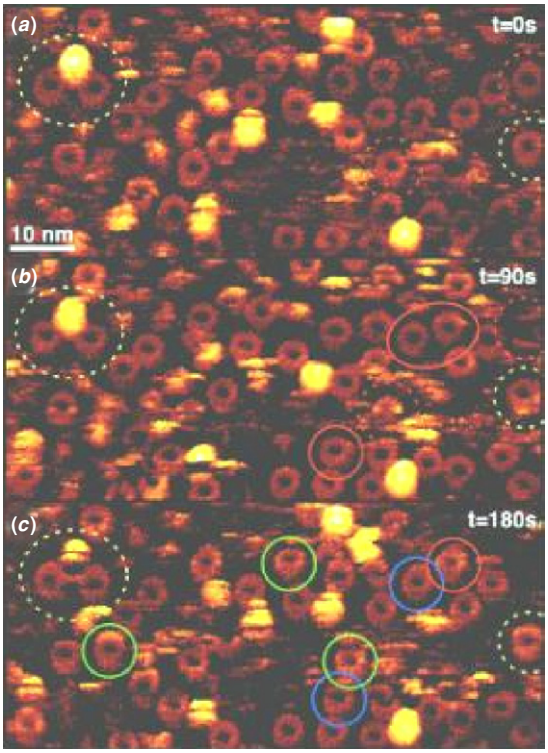

Figure 11. Diffusion of single rotors observed at a spatial resolution of ∼1 nm. (*a*) AFM topographs showing rotors assembled in the membrane. Subunits of individual rotors were observed directly in the raw data. (*b*) Same area imaged after 90 s. Individual rotors changed their location (continuous circles, outlined red in the online colour version) while others remained at their location (dotted circles, outlined yellow in the online colour version). (*c*) Repeated imaging of the same area after an additional 90 s. While some proteins moving in the previous images interrupted their movement (outlined blue) others continued (outlined red) or began to move. The circles dotted in yellow outline proteins, which did not change their location. Vertical brightness range of topograph, 3 nm. Reprinted with permission from [107]. Copyright 2003, Elsevier Science.

multilayers can be transferred by this method. Alternatively, lipid bilayers, which represent a unique model system for biological membranes, can be formed by fusing lipid vesicle on the substrate [113, 114]. AFM has been employed for studying films obtained both from a single-component lipid and from a mixture of different lipids. In these cases AFM is an excellent technique to characterize morphologically the obtained films, including the possibility of resolving defects on the nanometre scale and phase separation between different lipids. The possibility of identifying the presence of different phases is related to the high vertical resolution of AFM and the possibility of distinguishing areas with different mechanical or surface charge properties. The interest in lipid films is also connected to the possibility of using them as a support for immobilizing other biomolecules, either by inserting them in the membrane or by anchoring them at their top.

As far as morphological characterization of lipid films is concerned, the resolution obtained by AFM is at the molecular level [115–117]. In the case of dimyristoylphosphatidylethanolamine, bilayers were transferred on a mica surface and high-resolution images revealed the presence of spots separated by 0.5 nm from each other, which were attributed to individual headgroups of the phospholipid molecules [115]. The influence of the transfer surface pressure on the molecular-scale images of lipid layers has been investigated, finding a relation between the phase at the interface and the regularity of the imaged structure [118]. AFM offers the unique possibility of studying structural defects with nanometre-scale lateral resolution. This level of resolution allowed us to gain a deeper insight into defect formation mechanisms. The influence of chemical and physical external agents such as solvents, ions and temperature on the morphology of the supported layers has been elucidated in the case of symmetric and asymmetric bilayers. For example, it has been shown that alcohol may induce interdigitation in bilayers of dipalmitoylphosphatidylcholine [119]. The interdigitation can be deduced from a reduction in the thickness of the lipid bilayer and it was found to occur far below the threshold values for alcohol concentration established by other techniques such as x-ray diffraction. The effect of temperature on the topology of supported bilayers in relation to the gel/fluid phase [120], on the lipid-loss process [121] and on the ripple phase structure and kinetics of one- and two-component lipid bilayers [122] has been studied. The occurrence of the ripple phase, characterized by large-scale height modulation, is clearly recognized in AFM images due to the high vertical resolution of the technique.

Lateral segregation, due to phase separation, is easily observed by AFM in the case of single-component films, of a mixture of different lipids and in the case of the interaction of the film with other biomolecules. Bilayers in the solid phase differ from bilayers in the liquid phase, the former having a thickness greater than the latter. The presence of both phases organized in separated domains, when single-component lipid monolayers are transferred at a pressure corresponding to coexisting phases, has been observed [123]. AFM can be used to study the behaviour of lipid rafts, allowing a better resolution with respect to fluorescence microscopy [124, 125]. Lipid rafts are plasma membrane microdomains rich in glycosphingolipids and cholesterol forming a liquid-ordered phase surrounded by a liquid-disordered phase. Lipid rafts are also rich in certain types of proteins. These domains have a relevant biological function, being implicated in signalling pathways. In AFM images the rafts appear as islands protruding from the background by about 1 nm and proteins associated with the rafts are easily recognized [126].

In the case of mono and bilayers consisting of different immiscible lipids, phase separation can be visualized not only by topography but also by lateral force microscopy. Differences in lipid molecular packing and mechanical properties can be responsible for the contrast in lateral force between different domains both in air and in liquid (figure 12) [111, 127]. The different order degree may cause a difference in dissipation modes. Another mechanism of contrast formation in lateral force microscopy can be ascribed to different mechanical properties of different domains. This feature can be responsible for establishing a different contact area between the tip and the various domains. At the same time, the difference in mechanical properties may also account for a discrepancy between the measured and expected height difference of different domains. Also different surface interaction (steric, hydration, short range repulsion, etc) may influence the contrast mechanism both in contact mode and in

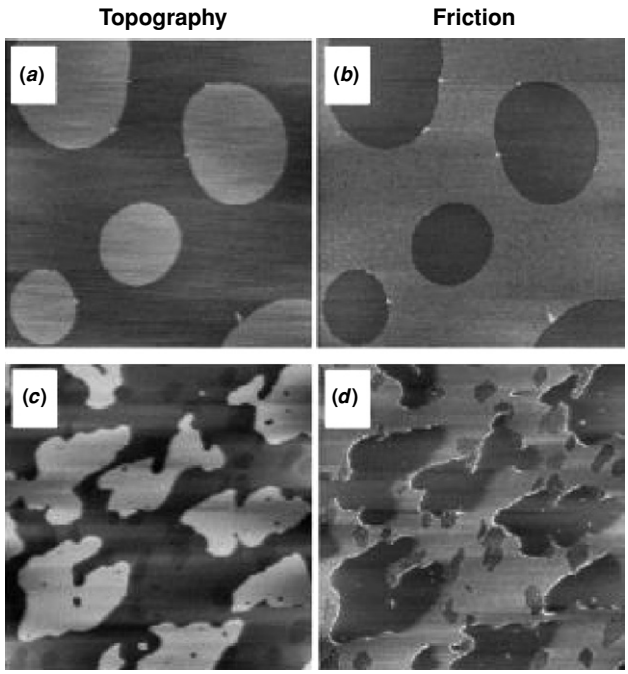

Figure 12. Topographic (*a*), (*c*) and friction (*b*), (*d*) images (15 × 15 μm^2) of monolayers in air (*a*), (*b*) and bilayers under water (*c*), (*d*) made of a mixture of saturated and unsaturated DOPE. Reprinted with permission from [111]. Copyright 2000, Elsevier Science.

lateral force microscopy in mono and bilayers composed of mixed lipid layers [128].

AFM studies on lipid membranes also include the role of membranes as support for inserting or immobilizing other biomolecules. The insertion in supported bilayers of small peptides such as gramicidin A and small model peptides [129, 130] and of lipopeptides such as surfactin-C_{15} [131] has been studied. As a support for immobilizing biomolecules, the lipid films have been used for anchoring DNA by exploiting positively charged lipids [51], proteins such as cytochrome c [132]. Moreover, negatively charged lipid films have been exploited as a substrate onto which several proteins crystallize allowing high-resolution AFM imaging [133].

3.4. AFM in cell biology

AFM applications in cell biology can be classified into several broad categories: imaging, micromanipulation studies, material property measurements and binding force measurements. The application of AFM to the study of mechanical properties and binding forces will be analysed in the following paragraphs after which the force-curve technique will be introduced and discussed. In this section we will focus on imaging applications. Imaging is the most straightforward application and a large number of cell types have been imaged by AFM taking advantage of the ease in studying biological samples under physiological buffer [134, 135]. Imaging of living cells has been coupled with controlled culture systems, enabling the possibility of continuous, long-term imaging. The possibility of controlling temperature and of continuous renewal of the culture medium by perfusion in order to prevent ionic strength variation due to evaporation, as well as fresh disposal of culture medium are basic requirements to be fulfilled to obtain long-term imaging of living cells [136, 137]. Moreover, AFM images can be collected together with light microscopy and fluorescence images to collect complementary information from the same sample area.

Whether the intermittent contact or the contact imaging mode represents the best way of imaging living cells is still a question under discussion. In the first mode lateral forces are greatly reduced in virtue of the intermittent contact between the tip and the sample which reduces the interaction time in comparison to the contact mode. Moreover, due to the high-frequency oscillation of cantilevers, the cellular surface may effectively become harder and less prone to deformation [138]. However, in some cases, the acoustic oscillations induced in the measuring environment might disturb living cells. Taking advantage of the phase signal, the intermittent contact mode can increase the amount of information that can be extracted from living cell images. The phase signal contrast is related to variations in material properties such as adhesion and viscoelasticity [139]. Being sensitive to local stiffness variations, phase imaging allows higher resolution imaging of the cellular surface [140] and a further improvement in resolution has been obtained by a positive feedback control of the cantilever oscillation amplitude [41]. Increasing up to three orders of magnitude the quality factor of the cantilever, imaging in the intermittent contact mode in liquid was performed at an interaction force below 100 pN. At the same time, the spectroscopic signal coming from the phase signal is greatly enhanced enabling us to distinguish areas with different dissipative interaction with improved resolution.

A typical contact-mode atomic force microscope image of a cell in physiological solution is reported in figure 13. The two images cover the same sample area and the left one is the usual height image, whereas on the right the corresponding 'error image' is reported. As a consequence of the loading force of the AFM tip on the cell membrane, the cell is indented and the membrane is pressed into the underlying cytosol. Stiffer structures under the membrane will be highlighted by this imaging mechanism. Large fibre structures are usually seen in AFM images of adherent cells such as fibroblast [141–143] and these fibres have been identified with stress fibres, i.e. bundles of actin filaments [144–146].

An important feature of AFM is the possibility of studying dynamic processes at high spatial resolution. However, time resolution is still rather low (technical advancements to increase scanning speed will be treated in the following), the acquisition time for one image being typically 1–3 min, limiting the time scale of observable phenomena to some minutes. Nevertheless, a broad range of dynamic biological phenomena have been studied by AFM, including the dynamics of actin filaments in living glial cells [141], the motility of cells [147] and the division of living cells (figure 14) [148]. The dynamic behaviour of intracellular structures has been examined for MDCK cells and the motion of particles along cytoskeletal elements has been followed [149]. For 3T3 fibroblasts, the extension and retraction dynamics of protruding edges has been followed, confirming that AFM imaging does not substantially perturb the imaged sample [144].

AFM appears to be a valuable tool also in the study of adaptation processes in response to mechanical stimuli of a cell, opening a new area in the field of biomechanics and

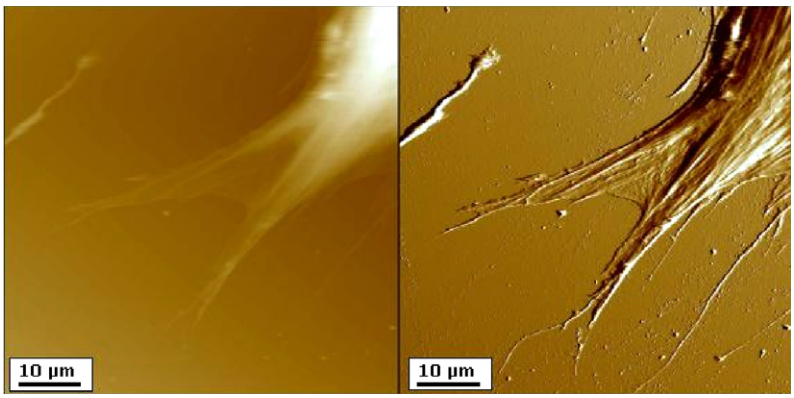

Figure 13. Topography (left) and error image (right) of a living human fibroblast grown on a glass slide. Note the enhanced resolution achieved in error mode where stress fibres are clearly visible.

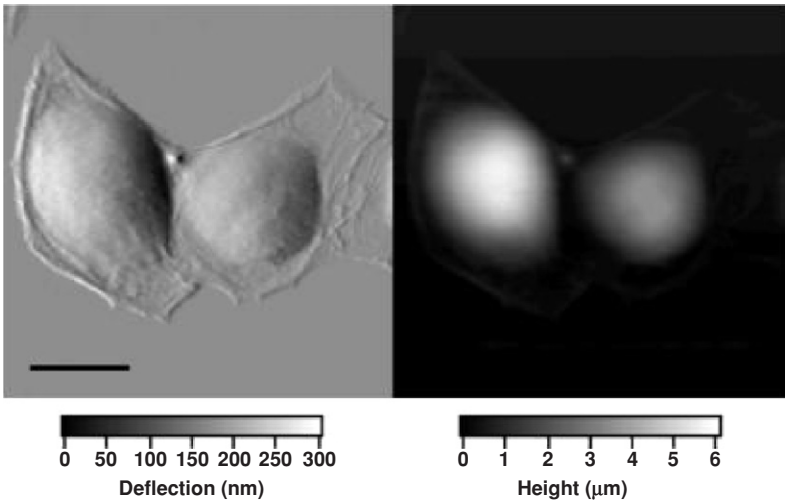

Figure 14. Error (left) and topography (right) images showing two daughter cells. Scale bar, 20 μm. Reprinted with permission from [148]. Copyright 2001, Nature Publishing Group. In electronic form: http://www.nature.com/ncb.

signal transduction [150]. Real-time variation in the height or volume of a single cell in response to a chemical stimulus has also been detected [151].

Atomic force microscopy has also been exploited to study the surface of bacterial cells, both after glutaraldehyde or drying pre-treatment and in hydrated conditions [152, 153], revealing details which have been impossible to detect by electron microscopy on native surfaces. Imaging the cell surface of microbial cells is a more demanding task with respect to animal cells, because they have no tendency to spread on solid surfaces. A valuable approach to study these cells consists in trapping them in porous filter membranes [154]. Using this technique the surface ultrastructure of living spores of the filamentous fungus *Phanerochaete chrysosporium* has been imaged [155], disclosing patterns of rodlets with 10 nm periodicity. AFM was also exploited to real-time image the enzyme digestion of the cell wall of *Saccharomyces cerevisiae* [156].

4. The force curve

The interest of the biophysical community in the potentiality of the AFM does not arise only because of the imaging capabilities of this technique, but also because of the possibility of studying intra- and inter-molecular forces. The operating tool of choice for this investigation is the force curve [157, 158]. The force curve consists in an approach–retract cycle between the tip and the sample during which the cantilever deflection is measured as a function of the relative motion. In figure 15 a typical force curve is shown. It can be divided into several regions. Starting from the right (region I) the AFM tip is far from the sample and no interaction is detected. Moving towards the left side of the plot (dotted curve), i.e. the tip is approaching the sample, no interaction is detected until the cantilever deflects towards the sample due to van der Waals forces (region II). These forces cause the tip to snap into contact with the sample. The 'jump to contact' point corresponds to the position where the gradient of the interaction force exceeds the cantilever spring constant. It is to be noted that at each position in the force curve the cantilever is deflected until its restoring force equals the interaction force with the sample, causing the system to be always at equilibrium. After the contact, approaching the tip further to the surface, a positive deflection of the cantilever arises (region III) due to repulsive forces. This is the contact region of the force curve, where elastic properties of the sample can be measured. Usually, the cantilever is moved

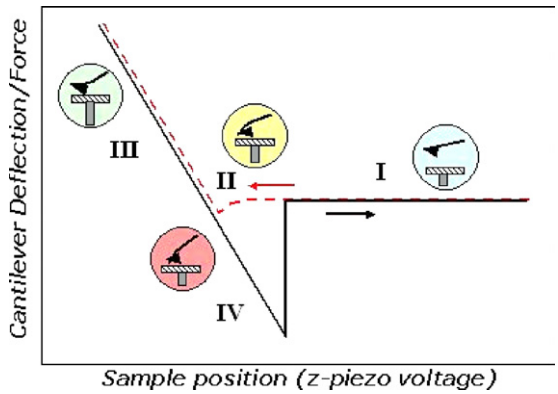

Figure 15. Scheme of a force curve with the different regions of the approach and withdrawal portions highlighted. The different regions are thoroughly discussed in the text.

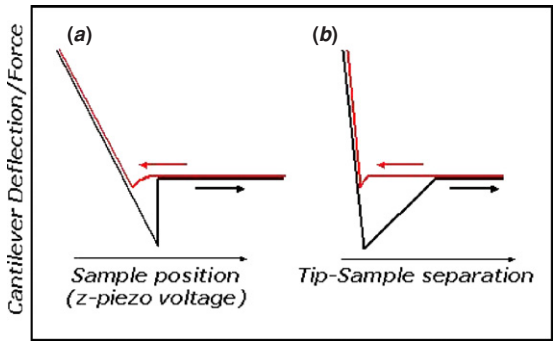

Figure 16. Correction of a force curve from the z-piezo movement parameter (*a*) to the tip–sample separation parameter (*b*). This correction is performed by subtracting the cantilever deflection from the z-piezo movement.

towards the sample until a preset force threshold is reached. After this happens, the movement direction is inverted and the cantilever starts moving away from the sample (solid curve). Initially, the behaviour of the cantilever during withdrawal equals that described for the approach, but, due to adhesion between the tip and sample, the cantilever starts to deflect negatively (region IV) until the adhesion force is overcome by the cantilever restoring force and the contact breaks. The hysteretic behaviour of curves measured in air is largely due to capillary forces arising from the thin water film wetting both probe and sample. It is clear that a large adhesion limits the range of information that can be obtained from a force curve, especially in the very interesting region of small tip–sample separation. However, the capillary forces can be greatly reduced by performing measurements in liquid, preserving at the same time a physiological-like environment for biological samples. The magnitude of the adhesion force can be used to compare interaction strengths between different molecules in a variety of environments [159–163]. To study the adhesion force between different chemical functionalities both tip and substrate are modified with adlayers terminating with an appropriate chemical group. After the tip–sample contact has been ruptured, they are again separated in a way that no interaction is measured (again region I). The atomic force microscope measures the cantilever deflection as a function of the z-piezo displacement, which differs from the actual tip–sample distance, to which force potentials refer, by the amount of cantilever deflection. However, by subtracting the cantilever deflection from the z-piezo movement, the actual force versus tip–sample distance can be recovered, as shown in figure 16 [164]. This transformation allows us to interpret the force curve in terms of force laws, which describe the force as a function of the probe sample separation.

In a force-curve cycle the cantilever deflection is measured, but it can be converted to force using Hooke's law:

$$F = -kd$$

where F is the force, k is the spring constant of the cantilever and d is the cantilever deflection. Different methods of measuring the cantilever spring constant independently have been developed. Essentially they may be divided into four categories: (1) methods based on the cantilever geometrical factors [165–168]; (2) methods based on the measurement of a static deflection applying a known force to the cantilever [169]; (3) methods based on measuring dynamical properties with different masses on the cantilever (added mass method) [170]; (4) methods based on the thermal noise of cantilevers [171, 172]. The last method is the most widely used. The cantilever is treated as a simple harmonic oscillator excited by thermal noise. However, the best accuracy in the measurement of the spring constant is around 15–20%, so the most convenient approach to improve accuracy in force measurements would be that of having an internal reference coming from a physical process known to take place at a well-defined force.

Using a cantilever with a very small spring constant, which can be as small as 10 mN m^{-1}, a resolution of 10 pN can be obtained in the measurement of interaction forces. The main noise sources come from thermal noise and from laser power (radiation pressure variations).

5. Force mapping

By collecting a set of force curves from many points on a sample, a two-dimensional map of the tip–surface interaction can be retrieved [164]. Typically, one force curve for each image pixel point is collected and the force curves may be analysed both individually and collectively. The force curves as a whole form a three-dimensional 'force volume' [164, 173, 174]. In the 'force volume' a two-dimensional matrix of force curves is acquired. Each force curve can be assigned to a defined pixel of a topographic image acquired at the same time as a result of the z-position at which a predefined force setpoint is reached. Recording all the force curves it is possible to recover a map of the cantilever deflection at a specific constant distance from the point of maximum applied force, which in the case of a rigid sample means a constant distance from the sample surface. In figure 17 a representative line scan of a force volume image is depicted. From the value of the cantilever deflection at a given distance from the point of maximum force, the elasticity map of the sample can be recovered.

As will be clear in the following, both the contact and out of contact parts of the force curve (approach and retract portions) can be exploited to create a map of the tip–sample interaction [175].

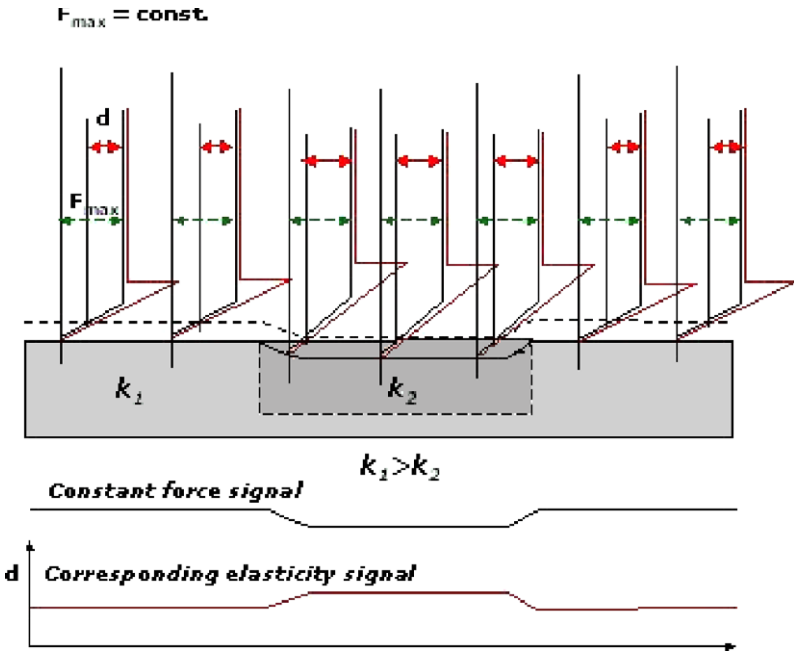

Figure 17. Operation scheme of the 'force volume' technique on a sample with regions of different elasticity ($k_1 > k_2$). A single line of the image is illustrated. A set of force curves is collected reaching always the same force (deflection) threshold (indicated in the scheme as F_{max}) using the no-interaction region as the zero force reference. The z-piezo extension needed to reach the threshold is different for the regions of different elasticity. The values for the z-piezo extension are exploited to obtain the usual constant force image, whereas by taking the cantilever deflection values (indicated as 'd' in the scheme) at a constant distance from the surface (dotted line near the sample surface) the corresponding elasticity image can be reconstructed. Note that the slope of the contact region in the force curves is different for the areas of distinct elastic properties.

Now we will concentrate on the specific interactions that AFM can detect and we will see how the force curve can be used to study both single-molecule forces and to create a map of the interactions with high lateral resolution.

6. Interactions measured by the atomic force microscope

The force curves can be rich in information from a biophysical point of view [175]. A useful classification of the data that can be extracted from force curves considers separately information derived from the approach part of the curve and from the retracting one.

6.1. Approach curve

Elasticity information on a biological sample can be obtained exploiting the approach part of the force curve. It is clear that, when the elastic constants of the cantilever and of the sample are comparable, once the tip is in contact with the sample, upon further approaching the sample will undergo indentation, resulting in a minor cantilever deflection for the same z-piezo movement with respect to an undeformable sample (see figure 18).

By measuring indentation at a given force, the local elasticity of the sample in terms of Young's modulus can be extracted, assuming a model for the tip–sample contact mechanics [173, 177–180]. A simple but not completely appropriate model is the Hertz model [181]. Usually, the Sneddon extension [182] to the Hertz model to account for the particular geometry of the indenting tip is used for the interpretation of AFM force curves. However, in AFM force curve experiments, especially in the case of soft cells, the assumptions of the Hertz model are not fulfilled. In particular, the axis along which the force is applied by the AFM tip is not perpendicular to the sample surface; lateral forces may be present and, usually, the examined samples are not isotropic. Studying cells, the cases in which the Hertz model fails are edges of cells where the very thin sample may cause the tip to feel the underlying stiff substrate or stress fibres representing very heterogeneous areas. Even if the retrieval of quantitative data is rather difficult, due to the criticality in the choice of the right model for the tip–sample interaction and to the heterogeneity of the biological samples, useful information, such as spatial and temporal variation of the mechanical properties, can be obtained. Moreover, maps of the local elasticity can be obtained by force mapping and spatial and temporal variations of the elasticity as a consequence of chemical treatments can be followed in real time as will be discussed in the section dedicated to force mapping of living cells. Not only the stiffness of biological samples can be measured, but also their viscoelastic properties [183–186]. In this case the sample under investigation can be rapidly indented and its slow recovery over a period of time is measured [187, 188]. The use of force–time curves, instead of force–distance curves, makes it possible to distinguish between the elastic and viscous contributions to the cantilever deflection. Using a low loading rate for the force-curve measurement the elastic behaviour predominates whereas, at high loading rate, the viscous properties are significant [187]. Several biological samples have been characterized from a mechanical point of view by means of AFM. They range from proteins [179] and chromosomes [189] to cells [179, 190].

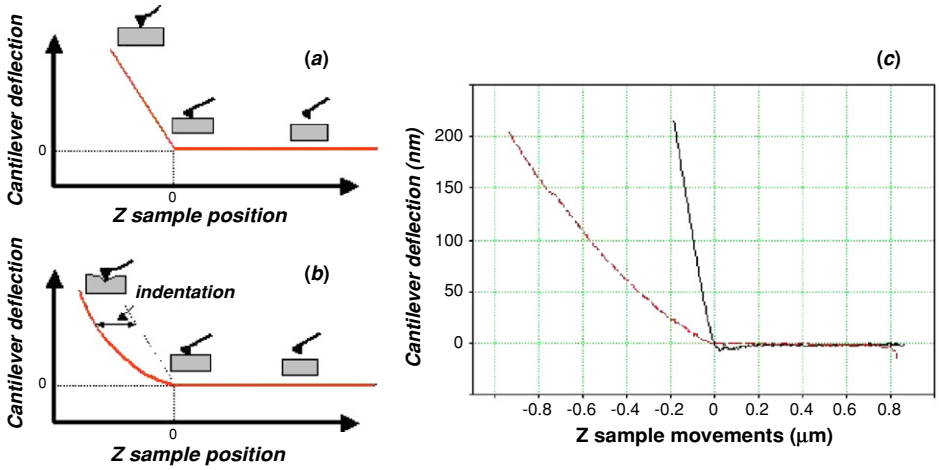

Figure 18. Indentation measurement by force-curve analysis. (*a*) Force curve on a rigid sample; (*b*) force curve on a soft sample. In this case the sample is indented and for the same cantilever deflection the z-piezo movement is higher than for the case of a rigid sample. (*c*) Comparison between two force curves performed on a living cell (dotted curve) and on the adjacent glass substrate (solid curve). The two curves have been aligned in order to have the same contact point.

The approach part of the force curve can also provide information on polymer brushing forces [191] and on the electrostatic surface charge of biological samples. Exploiting the force-curve analysis, Butt [192] measured the surface charge of purple membranes in solution using as internal reference the known surface charge of an alumina substrate. Information about the local surface charge can be obtained both by force-curve analysis and by comparing images obtained at different forces exploiting the differences in the apparent height of the imaged features [193].

As already outlined, coupling high precision in the measurement of forces with high lateral resolution in positioning the AFM tip, results in the possibility of mapping tip–sample interactions on a surface. The mapping can be realized exploiting both the approach and the retract portion of the force curve and in this section applications using the approach part will be considered.

The most important application of this technique regards 2D mapping of the viscoelastic properties of living cells [173, 179, 187, 194, 195]. Different regions of a cell present generally different elastic behaviour that can be mapped with a lateral resolution down to 50–100 nm. The low value for the lateral resolution on a living cell, compared to the high-resolution capabilities of the atomic force microscope, is a consequence of the low elastic moduli of living cells (1–150 kPa) [196]. The low stiffness of living cells leads to a high indentation of the tip in the cell membrane and a large contact area which limits resolution. Exploiting information from force-curve analysis, a height image of cells at zero loading force can be reconstructed. Unfortunately, determining the zero point (the point of the tip–sample contact) in the force–distance curve is not easy on soft samples because they do not show a sharp increase in the cantilever deflection. To overcome this problem, the equation describing the relation between the height of the sample, the cantilever deflection and the other sample parameters can be exploited to obtain a set of equations that can be inverted to obtain at the same time both the elastic modulus and the height offset representing the zero point. By fitting a contact mechanics model for the tip and sample to every force curve, the contact point between the tip and sample can be extracted [145] and used to reconstruct the zero loading force image.

The effect of a cytoskeleton-disrupting drug such as cytochalasin D was evaluated on fibroblasts [145]. The disaggregation of the F-actin network of the cytoskeleton by cytochalasin D led to a reduction of the cell stiffness, showing that the F-actin network plays a crucial role in maintaining the mechanical properties of cells. Figure 19 reports a time sequence of elasticity maps, together with topographical images (both height and deflection images to highlight the presence of stress fibres) showing the effect of a 10 μM cytochalasin D solution. The elasticity maps are reported in grey colour scale with darker areas corresponding to regions with lower Young's modulus. It is clear that 60 min after the drug was added, the average stiffness of the cell is greatly reduced. Another experiment stressed again the role of the F-actin cytoskeleton in maintaining the cellular mechanical properties [197]. In this case viniculin-deficient cells were compared, as far as elasticity is concerned, to wild-type cells. Viniculin being essential in the F-actin cytoskeleton linking to integrin receptors on the cell surface, the elasticity maps revealed, as expected, a lower Young's modulus for viniculin deficient cells.

In a fashion similar to a micro-detector, the atomic force microscope has been used to map in cardiomyocytes the mechanical pulse and its spatial variation [198]. The difference in the behaviour of single isolated cells and confluent layers has been characterized in this case, obtaining a more stable pulsing for the confluent layer case. Direct evidence of the driving force during cell division was given by Matzke *et al* [148]. The authors probed along a single line scan the stiffening of the cortex of adherent cultured cells during cell division. Using a sort of monodimensional force mapping they were able to detect a cortical stiffening over the equatorial region and a further stiffening as the furrow starts. It is to be noted that the AFM probing tip did not perturb the dividing cells as confirmed by video-microscopy used to correlate AFM data to the mitotic event.

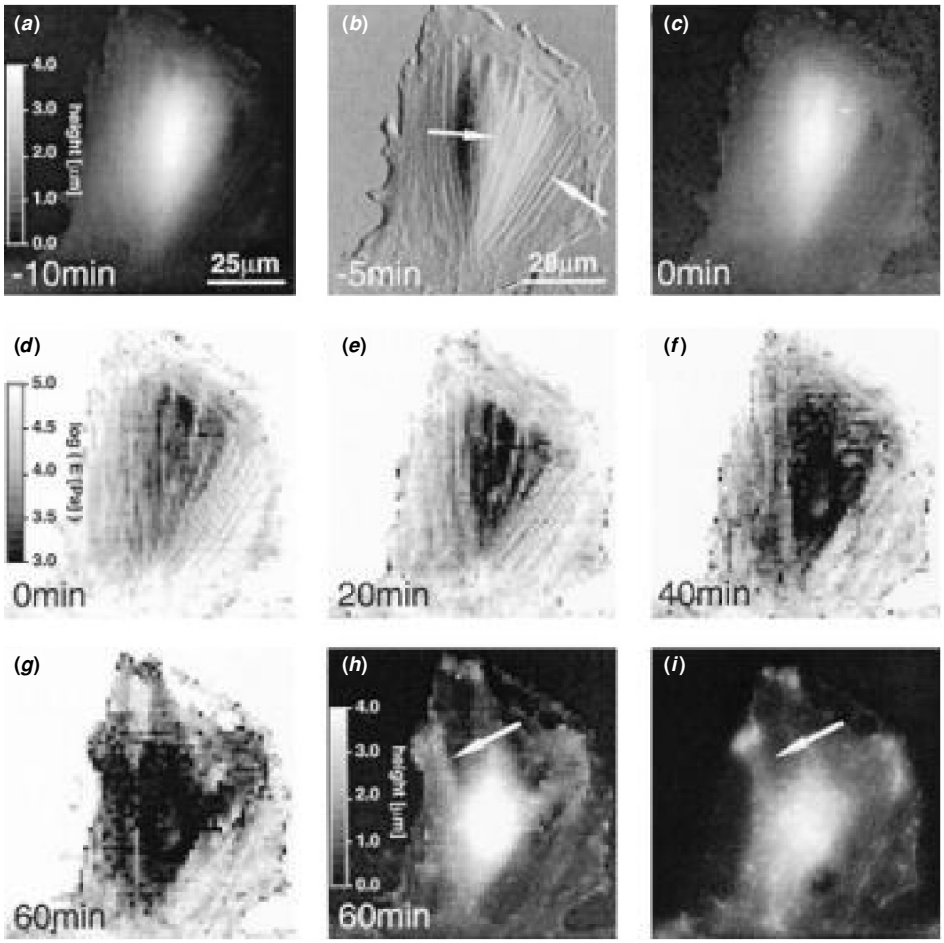

Figure 19. Time series of elasticity maps of an NRK fibroblast showing disaggregation of the actin network by 10 mM cytochalasin D and correlation with AFM and fluorescence images. (*a*) Contact AFM image. (*b*) AFM deflection image; stress fibres are depicted by arrows. (*c*) Height image at zero loading force calculated from the reference force map. (*d*) Corresponding reference elasticity map. (*e*), (*f*) Young's modulus decreases gradually within 40 min. (*g*) Elasticity map and (*h*) height image at zero loading force obtained after 60 min showing strong segmentation of the cytosol. (*i*) Corresponding fluorescence images to identify structures in (*g*) and (*h*) as clots of actin. The arrow in (*h*) points to a very flat region (500 nm) that correlates with a region devoid of f-actin (*i*, arrow). Reprinted with permission from [145]. Copyright 2000, Biophysical Society.

6.2. Retract curve

The retract portion of a force curve can give access to a wide range of inter- and intra-molecular interactions at the single-molecule level. We will divide this section into two parts: the first part dedicated to intermolecular interactions, in particular recognition events between biological partners, and the second one dedicated to intramolecular forces concentrating on the mechanical properties of DNA and on the mechanical unfolding of proteins.

6.2.1. Intermolecular interactions. As already described, the retract curve can give information on the adhesion force between the tip and sample and adhesion maps on a sample surface can be obtained by an approach called chemical force microscopy [27, 199]. If on the sample surface there is a molecule and the tip is functionalized in order to expose a partner suitable to specific interaction with it off its surface, the ligand–receptor interaction can be measured by exploiting the rupture force in the retract portion of the force curve. When the tip and the surface are brought into contact, the molecular partners interact. Upon cantilever retraction, the bonds previously formed are disrupted and the typical rupture force is measured. In all these experiments, it is important that the strength of the intermolecular bond established between partners be weaker than those used for anchoring them to the surface. To this end, specific techniques have been developed to immobilize biomolecules on surfaces by bioconjugation chemistry preserving their recognition capabilities [200–202]. In an elegant experiment by Grandbois *et al* the strength of a single covalent bond has been measured [203]. The sulfur–gold bond, which is often exploited to immobilize biomolecules on surfaces, is able to withstand forces up to 1.4 nN. If the biotin–avidin interaction force is considered, its strength is about 200 pN at a loading rate of 10^5 pN s^{-1} [204], therefore the sulfur–gold covalent bond would be stronger than six biotin–avidin interactions, enabling stable force-curve measurements without running the risk of detaching the molecular partners from the respective surfaces. The statistical analysis of data is of great importance to extract information about the single-molecule binding interaction. Usually, a distribution of the number of rupture events as a function of the

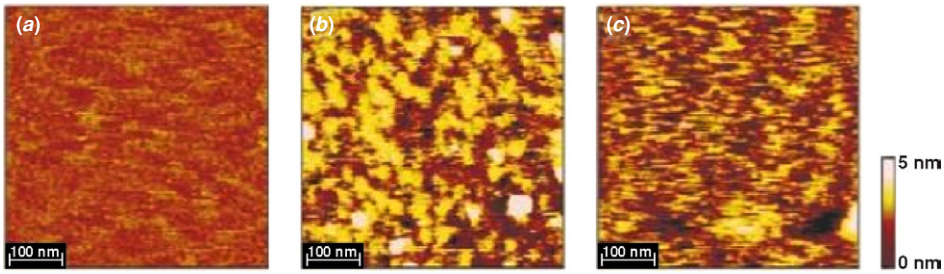

Figure 20. (*a*) Topography image of a lysozyme multilayer. Image size was 500 nm. (*b*) Multilayer recognition image. Imaging was performed using an AFM tip carrying one half-antibody with access to the antigens on the surface. The bright dots representing recognition profiles indicate lateral positions where antibody–antigen recognition occurred. (*c*) Multilayer block image. The image was obtained with the same half-antibody tip and conditions as in (*b*) in the presence of free antibodies in solution. Reprinted with permission from [231]. Copyright 1999, Nature Publishing Group. In electronic form: http://www.nature.com/nbt.

rupture force is obtained. The presence of a quantum of rupture force is the indication that a single-molecule interaction is measured, the multiples of the binding force being the result of coincident breakage of several bonds. Moreover, when a retract curve presents several rupture events, the last one represents most likely a single bond breakage. To avoid the establishment of too many bonds between molecules on the tip and molecules on the surface, the density of molecules on both surfaces must be kept at minimum. With this aim, the use of biofunctionalized carbon nanotubes as tips will enable a remarkable advance in the technique [23], allowing for only a few molecules, possibly just one, on the tip. In order to avoid misinterpretation of the results, some control experiments have to be run. For example, if the specific partner of the surface immobilized biomolecule is inserted in the medium, this will block the partner on the surface and no rupture event has to be detected in the measurements.

Several ligand–receptor pairs have been studied, including biotin–(strept)avidin [23, 205, 206], antibody–antigen [200, 207–212], the interaction between complementary strands of DNA [213–219] and interactions between the protein of the cell membrane and specific partners on the AFM tip [220, 221].

Also in the case of the retract portion of the force curve the ability of the AFM to detect specific biological interaction and recognition events can be coupled with the imaging capabilities to map the lateral distribution of binding sites and the binding characteristics at the same time. The so-called adhesion mode or affinity mode imaging is obtained [173, 212, 222–224]. In particular applications, also forces resulting from specific recognition events in lateral force microscopy can be used as a contrast parameter [217].

The biotin–avidin couple represents undoubtedly the model system for the binding force measurements by AFM tips. The values of the interaction force obtained by different laboratories agree well, reinforcing the reliability of these force spectroscopy measurements. The biotin–(strept)avidin system has also been the test system for demonstrating [225] the exponential dependence on force loading rate of the rupture force predicted by Evans and Ritchie for weak non-covalent bonds [226]. The presence of different regimes of loading rate was correlated with the number of activation barriers in the unbinding process. Moreover, by using a streptavidin mutant, the molecular region determining the activation barrier was identified [225]. It is clear that, by varying the kinetics of the ligand–receptor unbinding, other information on the ligand–receptor bond is accessible by force spectroscopy. Affinity rate constants together with energy barriers, equilibrium dissociation constant and bond width can be estimated [200, 227–229]. Adhesion images exploiting the biotin–streptavidin binding have been obtained by Ludwig *et al* [230]. They were able to obtain a topographic and adhesion image, at the same time, of a surface patterned with streptavidin and BSA. Blocking the surface with free biotin in solution the topographic image was retained whereas the adhesion image was lost.

Whereas a biotin–avidin couple has a high binding affinity ($K_d = 10^{-15}$ M), antigen–antibody interactions are characterized by a lower binding affinity and a greater binding sensitivity to steric effects. These factors have been overcome by using flexible cross-linkers to link either the antigen or the antibody to the tip [200, 209, 210]. The flexible linker endows the molecular partners with sufficient mobility to overcome problems of steric hindrance or misorientation. In these cases, usually a polyethylene glycol (PEG) spacer is used, because it is a water-soluble and non-adhesive polymer. When the coupling of the antigen or antibody to the tip is realized by means of such a cross-linker, the rupture event is not characterized by an immediate detachment on the retract portion of the force curve, but a delayed event is found which follows the stretching of the spacer. Adjusting the concentration of antibody used to functionalize the tip, a single-molecule binding event can be studied, allowing us to discern both the binding sites of the antibody and the probability of the rupture event as a function of the lateral position of the antibody over the antigen. Raab *et al* [231] were able to map lysozyme molecules on mica using anti-lysozyme antibodies tethered to the tip by a PEG spacer (figure 20). Using the intermittent contact mode in which the cantilever is magnetically oscillated and the tip is functionalized with antibodies, they were able to localize antigens on the mica surface with 3 nm lateral resolution. The recognition signal comes from the extra damping of the oscillation when a specific recognition event between the molecular partners on the sample and the tip occurs. This method allows for a high lateral resolution in determining antigen position, even if a quantitative measurement of adhesion forces is much more difficult to obtain.

Force spectroscopy experiments on DNA pertain for some aspects to intermolecular interactions, in particular as far as the unzipping forces are considered. Usually one strand of

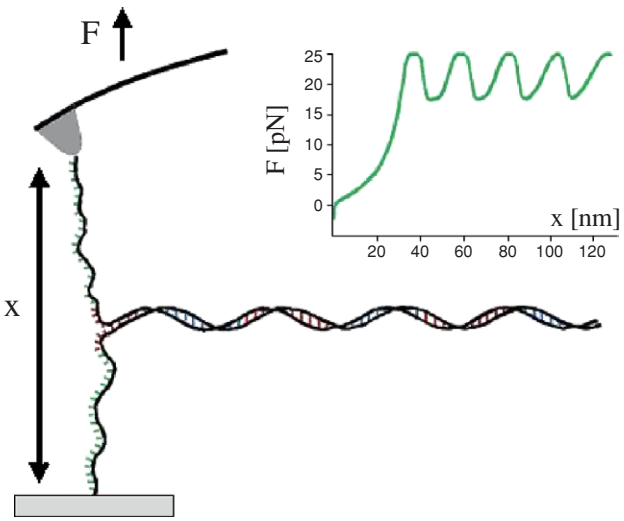

Figure 21. Complementary DNA oligonucleotides are chemically attached to an AFM tip and a glass surface. As the tip is brought into contact with the surface a double strand forms, which can subsequently be unfolded upon retraction of the tip. Reprinted with permission from [234]. Copyright 2003, American Chemical Society.

DNA is immobilized on the tip and the other on the surface. Upon tip–surface contact, the two strands can hybridize and upon retraction the pull-off force provides an estimate of the pair binding force. Experiments on the interaction force between complementary strands of DNA immobilized on tip and surface report different values for the interaction force per base pair [213–215]. The discrepancy may be due to an interplay between specific and unspecific forces [232]. Using a cross-linker between the strands and the surfaces it has been possible to study the unzipping force between complementary strands of DNA getting rid of problems connected to unspecific forces [214]. The rupture force of duplexes with different numbers of base pairs was found to scale linearly with the logarithm of the pulling velocity and the separation of the energy minimum from the barrier increased linearly with the number of base pairs, proving the single barrier character of the unzipping process and a non-linear dependence of the unbinding forces on the number of base pairs. Also the dependence of the force-induced melting threshold on the ionic strength, temperature and sequence has been investigated, showing also that after some base-pair breaking, the molecule may recombine to the double-helical conformation upon relaxation [233]. Using a different experimental arrangement, a DNA oligomer was stretched by pulling the 5′ and 3′ ends of the two strands (figure 21) [234]. In this experiment dsDNA molecules with repeating blocks of ten pure GC and ten pure AT base pairs were unzipped obtaining, as expected from simulation predictions, variations in the unzipping force of 5 to 10 pN according to the different base pairs involved. In this work ten-base-pair resolution has been obtained in the force unzipping and it represents the best resolution to date. The unbinding force dependence on the presence of sequence-specific and unspecific intercalating agents such as 3,6-diaminoacridine and ethidium bromide has been explored [235]. The intercalating compounds lead to a reduction of the unbinding force, probably due to a conformational change of the DNA duplex to accommodate the molecules.

Structural transitions of the DNA duplex that precede the unbinding events will be discussed in the context of intermolecular forces.

Of great importance are the investigations of the interaction between biomolecules on the AFM tip and the corresponding partners at the cell membrane. These experiments are challenging because molecules in the cell membrane can be easily displaced from their native location upon pulling the tip or they may be present in too low a density to be detected. However, the possibility of detecting and mapping the distribution of receptors on the membrane of a living cell by force spectroscopy has prompted several works on this aspect [236, 237]. The binding force between an arginine-glycine-asparagine (RGD) peptide and integrin, its cognate receptor, has been measured on living cells [220]. The binding force appears to depend not only on the type of integrin and its activation status, but also on the spatial conformation of the RGD containing sequence of the peptide or protein. In another experiment, the role of cross-linking of surface receptors in increasing their binding force has been demonstrated [238]. In this work concanavalin A was coupled to the AFM tip and the binding force to its receptors on the surface of NIH3T3 cells was measured before and after the receptors were fixed by glutaraldehyde or 3,3′-dithiobis(sulfosuccinimidylpropionate). Immobilized membrane proteins are less prone to diffuse laterally and this lack of mobility leads to a cooperative binding (the term cooperative means simultaneous breakage of multiple bonds) and hence to an increase in receptor binding force. In a sort of assay test, force mapping by atomic force microscopy was used to distinguish red blood cells of different ABO groups [221]. In this experiment a lectin functionalized tip is exploited to recognize a glycolipid present on the membrane of group A cells. The unbinding force map was able to construct an affinity map identifying the A cells from the O cells lacking the molecular partner.

6.2.2. Intramolecular interactions. The AFM can be very useful in studying also intramolecular interactions, which are, in general, weaker than those associated with bond rupture events. Mechanical properties and information about the conformation of single molecules can be extracted by stretching molecules bound between a tip and a substrate [239, 240]. Theories related to the thermodynamics of polymers can be used to fit the experimental data and extract information about the elasticity of single molecules [241]. Moreover, parameters obtained from the fitting can be used to establish if a single molecule or more than one molecule has been stretched. Elasticity implies that when a polymer is stretched between the tip and the substrate, restoring forces arise. The first restoring force that develops upon stretching a polymer is due to the entropy reduction as a consequence of the reduction in conformational degrees of freedom [242]. Increasing the pulling force, conformational changes can occur to the molecule, leading to bonds stretching and twisting (enthalpic elasticity) [243]. These effects endow the force–extension curves with specifically recognizable features. Major research efforts have been devoted to stretching DNA, to

identify conformational changes preceding strands unzipping, and to stretching proteins with the aim of shedding light on some aspects of their unfolding process.

Understanding DNA mechanical properties is of great importance for their implications in many biological processes. In the low extension–force regime (<65 pN) the restoring force is mainly entropic in nature and the DNA can be described by the 'worm-like chain' (WLC) model, in which the conformation of a polymer chain is considered as a continuous curve with constant bending elasticity [242, 245–247]. Fitting the WLC theory to the experimental curves values for DNA, persistence and contour lengths can be evaluated [248]. Increasing the stretching force, DNA undergoes conformational changes in which the stacking interactions of DNA bases are lost (B–S transition) resulting in extension of the molecule beyond its contour length [249]. The typical signature of this conformational change is the presence of a plateau in the force–extension curve, due to the fact that very little additional force is involved in the stretching of the molecule up to 1.7 times its B-conformation contour length [216, 250–252]. The presence of the plateau in the force–extension curve of DNA has also been interpreted in terms of a mere melting of the double helix, in which the base pairs break as the DNA unwinds during the transition [253, 254]. By stretching DNA beyond the B–S transition, a new conformational transition appears at about 150 pN [250]. Beyond 150 pN the double-stranded DNA is separated into the two strands, one of which remains bound between the tip and surface and, upon further stretching, the force increases steeply with extension. It was found that the B–S transition occurs on a time scale much faster than that of the cantilever movement (typically on the μm s^{-1} scale) assuring a complete reversibility to the transition, whereas the melting transition occurs on a much slower time scale and is not completely reversible. Indeed, if the DNA molecule is relaxed, inverting the movement of the cantilever, after the second conformational transition has occurred, the force–extension curve follows a smooth trend, representative of single strand DNA mechanics [255]. This hysteretic behaviour is indicative of a force-induced melting transition by which the double-stranded DNA is divided into two single strands. Moreover, the first transition was found to be independent of the pulling velocity, whereas the second transition depends on the pulling speed. As a general rule, different results may be obtained stretching DNA polymers, depending on the details of the experiment, in particular the way of binding the molecule to the substrate and the resting time before starting to retract the cantilever [233]. The effect on the force–extension curve of different drugs bound to double-stranded DNA has been investigated [247]. It has been found that the force–extension curves present features characteristic of the particular drug–DNA interaction mode and of the drug concentration. Also the mechanical properties of RNA have been investigated by AFM force spectroscopy obtaining a different behaviour with respect to DNA [256].

Force spectroscopy has been largely applied to the study of the mechanical properties of individual proteins by exploiting force as a denaturant agent. In the following we will present an overview of the potentiality of this technique in this field of investigation, but several outstanding reviews dedicated to single protein force spectroscopy may be found in the literature [257–259]. The force spectroscopy technique for studying protein folding can provide complementary information with respect to bulk solution experiments. First of all, experiments refer to single molecules instead of giving averaged information as for the case of bulk experiments. Having a well-defined reaction coordinate, defined by the direction of the exerted force, force spectroscopy data allow us to explore a different energy landscape of the unfolding process and are good examples to be compared with molecular dynamics simulations dealing with single molecules. The unfolding pathways for chemical and thermal unfolding are found to be different from the force-induced unfolding pathways even if they may have a similar barrier.

Usually, a layer of proteins is either adsorbed to the substrate or is covalently attached to it. Approaching the tip to the substrate, one or more proteins can attach to the tip simply by adsorption. Retracting the tip from the substrate the protein starts to be extended. From a technical point of view, in order to be able to quantitatively interpret the force curve related to an unfolding event a single protein has to be picked up (by a 'fishing' approach) by the tip. If multiple molecules attach to the tip it is impossible to deduce useful information from the force curve. To this end, the concentration of protein adsorbed on the surface has to be finely tuned in order to have a reasonable probability of picking up a single protein. The ideal experiment would be that in which the tip picks up a single fully folded protein at the opposite end with respect to the protein end tethered to the substrate. However, this is rarely the case; rather the tip can interact with the protein at any point along its contour length. In order to make quantitative measurements several sources of systematic errors have to be controlled. The main error source comes from the spring constant calibration of the cantilever, which, in the most favourable cases, is of the order of 10–15%. Other sources of error come from drift of the cantilever or the whole experimental set-up. The dependence of the unfolding force on pulling speed requires a set of experiments to be performed at different retract speeds of the cantilever. At high speed in liquid, viscous drag on the cantilever can introduce errors and the technique would greatly benefit from the use of short and low noise cantilevers. The study of pulling-speed dependence of the unfolding force opens the possibility for extracting kinetic information from these experiments. However, the range of pulling speed that can be probed by AFM studies is limited and force spectroscopy studies performed with techniques enabling a wider range of pulling speeds might highlight different transition states.

The first experiments concentrated on the giant muscle protein titin, which contains a large number of immunoglobulin domains [240]. When a protein is stretched between the tip and the substrate, if more than one domain is comprised between them, a saw-tooth pattern is found as schematized in figure 22. This behaviour is due to a series of entropic and enthalpic contributions, the first ones being related to the initial stretching of the protein and to the stretching of unfolded domains, resembling a common polymer stretching, and the second ones being related to the unfolding of individual domains. Starting from position 1 in figure 22(*b*) the protein is elongated and the restoring force,

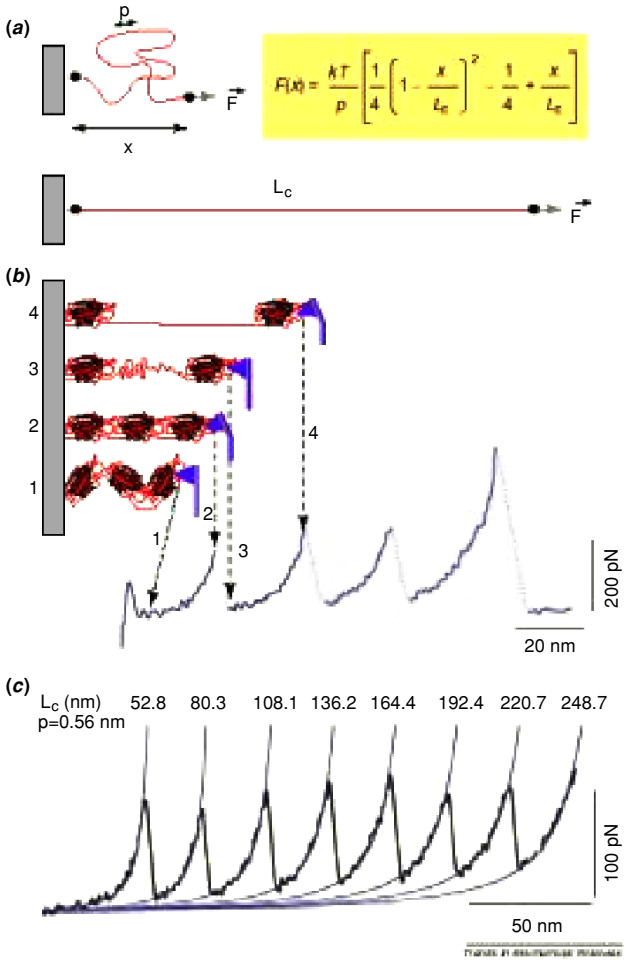

Figure 22. The entropic elasticity of proteins and domain unfolding. (*a*) The entropic elasticity of proteins can be described by the WLC (worm-like chain) equation (inset), which expresses the relationship between force (F) and extension (x) of a protein using its persistence length (p) and its contour length (L_c). k is Boltzmann's constant and T is the absolute temperature. (*b*) The saw-tooth pattern of peaks that is observed when force is applied to extend the protein corresponds to sequential unravelling of individual domains of a modular protein. As the distance between substrate and cantilever increases (from state 1 to state 2) the protein elongates, generating a restoring force that bends the cantilever. When a domain unfolds (state 3) the free length of the protein increases, returning the force on the cantilever to near zero. Further extension again results in force on the cantilever (state 4). The last peak represents the final extension of the unfolded protein prior to detachment from the AFM tip. (*c*) Consecutive unfolding peaks of recombinant human tenascin-C were fitted using the WLC model. Reprinted with permission from [257]. Copyright 1999, Elsevier Science.

entropic in nature, deflects the cantilever (position 2). When the force exerted by the cantilever is such to unfold one domain, a sudden increase in the chain length makes the cantilever go back to its undeflected state (position 3). The denatured portion of the protein undergoes entropic stretching up to the position where another domain is unfolded (position 4). Each individual domain is responsible for one peak in the force curve. Usually, the peaks are in increasing force order due to the fact that more unstable domains with lower unfolding barrier unfold first. A great advance has been made in the interpretation of force curves by introducing protein engineering techniques in order to have proteins with a known and adjustable number of identical domains. This technique overcame the uncertainty in assigning each force peak in the force curve to a specific domain in the protein [260].

Another protein domain that has been studied is the FN-III domain of the extracellular matrix protein tenascin [261]. This domain presents an unfolding force significantly lower than the unfolding force of Ig domains (about 130 pN for FN-III domains, 150–300 pN for Ig domains). Another useful parameter that can be extracted from force curves is the number of amino acids forming the unfolded domain. This information can be derived from the distance between peaks which corresponds to the contour length increase, upon single domain unfolding. When α-helical domains are unfolded, such as in the case of the cytoskeleton protein spectrin [262], a lower unfolding force is found (25–35 pN), suggesting a relationship between the particular protein domain and the mechanical strength needed to unfold it. When β-barrel domains, such as the Ig-like domains of titin, are unfolded, much more force is needed to break the numerous hydrogen bonds stabilizing this structure, with respect to α-helical domains, in which only hydrophobic interactions stabilize the domain structure. The role of sequence and topology in determining the mechanical stability of domains can be elucidated by AFM force spectroscopy investigations. For example, two Ig domains, I27 and I28, which have low sequence identity but similar topology, present very different mechanical strength, highlighting the importance of side chain interactions for the mechanical stability [263]. Moreover, by exploiting protein engineering techniques, it is possible to show how sequence changes can alter the mechanical properties of proteins [264]. In AFM unfolding experiments the presence of unfolding intermediates may be observed by careful analysis of force curves [265]. Molecules with a role in cell attachment and stress transfer have been studied by force spectroscopy, comparing the unfolding trajectories when intradomain disulfide bonds are intact or disrupted by chemical reduction using the reducing agent DTT [266]. It was found that under reducing conditions the domains fully unfold through an intermediate folded state, whereas, when the disulfide bonds are intact, only a partial unfolding is observed. These studies highlight the role of disulfide bonds in regulating unfolding under tension.

AFM force spectroscopy experiments on proteins have been coupled to the imaging capabilities of AFM. Müller *et al* [267] imaged a two-dimensional bacterial surface layer of HPI before and after a pulling event. The pulling event, which was preceded by a local increase in the tip–sample force to ensure an attachment of a protomer to the AFM tip, presented a force curve with multiple peaks and subsequent imaging of the same area allowed us to determine which bacterial pore was extracted (figure 23). By this experiment the intramolecular forces of individual proteins have been determined. Also sequential unfolding of transmembrane domains of bacteriorhodopsin embedded in its native purple membrane has been studied, elucidating also the role of pH, temperature and point mutations on the stability of individual transmembrane domains [268].

Protein unfolding experiments by AFM are constantly increasing their popularity and studies are now facing more

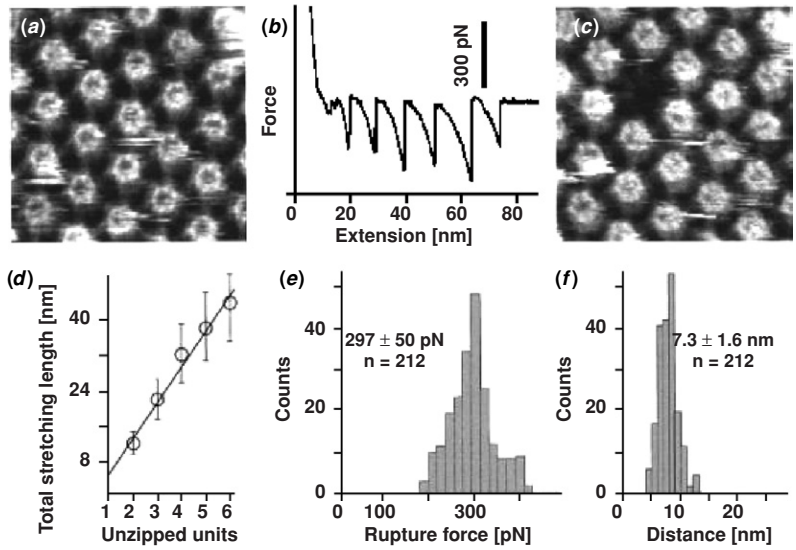

Figure 23. Multiple protomers can be sequentially pulled out of the HPI layer. (*a*) Control AFM topograph of the inner surface of the HPI layer. (*b*) The force–extension curve recorded from this inner surface region shows a saw-tooth pattern with six force peaks of about 300 pN. (*c*) The same inner surface area imaged after recording the force curve; a molecular defect corresponding to the size of a hexameric HPI protein complex has clearly been created. (*d*) Relation between the total stretching length and the number of force curve peaks. The straight line obtained indicates a direct correlation between the force peaks and number of extracted protomers. (*e*) Histogram showing the adhesion forces measured from 212 force–extension curves. The peak is at 297 ± 50 pN. (*f*) Stretching distances between protomer disruption events have a sharp peak at 7.3 ± 1.6 nm. The full grey-level range of the topographs corresponds to 3 nm. Reprinted with permission from [267]. Copyright 1999, National Academy of Science, USA.

relevant biological problems from the initial model cases. The use of force as a protein unfolding agent is of great relevance in particular for those proteins which have a mechanical function in nature. In these proteins individual domains might unfold and refold executing mechanical functions, consequently, force spectroscopy, providing information on the force-induced unfolding of single protein domains, offers new insights into the function of mechanical proteins. α-helical domains have shown to unfold upon forces lower than those required for β-sandwich domains, in accordance with the mechanical stabilization by hydrogen bonds between β-strands. In any case, even for protein which does not have a mechanical function, force spectroscopy investigations can give complementary information with respect to thermal and chemical unfolding. Technical developments, in particular the force-clamp technique, which is able to apply a constant force over time, will allow us to study also protein refolding [269, 270].

7. Perspectives

From the survey included in the previous paragraphs it is evident that AFM is now a commonly used technique in the field of biophysical research. During the last decade it has evolved from a purely imaging tool to a technique which can provide information on interactions between single molecules, which can probe mechanical properties of biological samples at the nanometre scale and can also help in manipulating single molecules. The possibility of studying samples in solution enables us to image biological processes in real time at high spatial resolution. In the following we will summarize the most promising ongoing technical developments as well as some of the most charming research opportunities that AFM will enable us to tackle in the near future.

7.1. Cantilevers and tips

As already noted, the force sensor, including the cantilever and the tip, is the heart of the AFM and it is clear that technical developments are mainly focused on improving the performances of this component. The introduction of carbon nanotube tips [21] has remarkably increased the performances of AFM as far as lateral resolution is concerned and the field of structural biology is starting to benefit from this advancement. However, a great contribution from carbon nanotube tips is also expected in the field of chemical sensing imaging and force spectroscopy. Indeed, nanotubes, at variance with normal AFM tips, have a well-defined surface chemistry and can be specifically functionalized, even with single biomolecules, only at their very ends. In this way, chemical and affinity mapping can be executed with previously unmatched resolution [21, 23] (figure 24).

Other tip modifications will increment the amount of chemical and biochemical information derivable from atomic force microscopy. It has been shown that valinomycin/polyvinyl chloride-modified AFM tips are sensitive to specific ions, allowing us to localize ion pores [271] and to measure ion concentration in a localized region of a surface [272].

Increasing the scanning speed of AFM to improve time resolution is strictly connected to the development of new types of cantilevers. The speed in atomic force microscopy is limited by mechanical constraints [273]. Rapid imaging in contact mode of a biological sample would drastically increase damage and degradation due to the huge dragging force. As far as AFM biological applications are concerned, the major efforts have to be devoted to speed up the scanning process in intermittent contact mode. In order to maintain a high signal-to-noise ratio, cantilevers with higher resonant

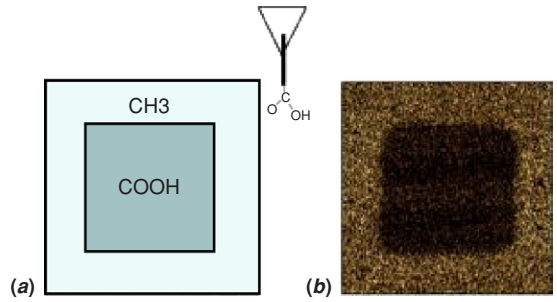

Figure 24. Chemical force microscopy by carbon nanotube tips: (*a*) scheme of a pattern made up of regions with different chemical functionalities. (*b*) tapping-mode image of the pattern in (*a*) obtained with a carboxyl-terminated nanotube tip. The contrast is due to the different interaction of the tip with the functional groups on the surface. Reprinted with permission from [21]. Copyright 2001, Elsevier Science.

frequencies are needed, while their spring constant should remain constant. One way to obtain all these properties is to reduce the mass of the cantilevers, making small cantilevers in order to combine high resonance frequency with small spring constant. Short cantilevers (9–40 μm), endowed with MHz resonance frequency, have been fabricated [274] allowing us to create a sequence of images in liquid at 80 ms intervals [275]. The spreading of these cantilevers to a commercial level, along with the development of optical detection systems for cantilever deflection suitable to deal with this tiny cantilever size, will increase the number of biophysical processes studied both at high spatial and high temporal resolution (video AFM). Together with working on the dimension of the cantilever, one has to work on the dynamic behaviour of the moving parts such as the piezoelectric scanner, which represents the most severe obstacle to high speed imaging. One possible solution to overcome the problems connected to the resonance frequency of the scanner would be to integrate a piezoelectric actuator on the cantilever. However, this solution leads to large spring constants for the cantilever, resulting in possible damage of biological samples. In some cases, the use of smaller high-frequency piezo segments to the moving z-scanner has been introduced [276]. Another limiting factor for high speed imaging in the intermittent contact mode is the time it takes for the oscillating cantilever to change amplitude [277]. A remarkable breakthrough in this sense has been the introduction of an active damping circuit to increase the speed at which the cantilever can respond [278].

As a general comment, the investigation of biological samples would greatly benefit from higher imaging speed. Insights into the mechanisms biomolecular machines exploit to perform their biological functions could be obtained by high speed AFM. High speed AFM will allow us to follow the dynamics of biological processes at the nanometre scale.

Small cantilevers can also be exploited in force spectroscopy experiments. In this case the advancement with respect to conventional cantilevers is in the reduced coefficient of viscous damping which allows the measurement of smaller forces at large bandwidths [279, 280].

The implementation of tip arrays appears also to be very promising, since they will increase drastically the accessible scan area and will enable simultaneous mapping of distinct sample properties if tips functionalized with different chemical groups will be used [281].

7.2. Combination of different techniques

AFM apparatus can be naturally coupled with other techniques to increment the amount of information obtained out of a single scan. The combination of different techniques will endow atomic force microscopy with analytical probes, which are now lacking in conventional AFM investigations. AFM has been successfully integrated with the scanning ion conductance microscope (SICM) obtaining at the same time a topographic image and an ion conductance map [282]. The AFM allows us to maintain a constant distance from the sample surface while measuring the ion flux. Fluorescence detection has already been combined with atomic force microscopy; special fluorescence techniques such as fluorescence resonance energy transfer (FRET) seem particularly appealing for integration with AFM since such a combination could enable us to follow in real time a number of conformational changes at molecular level (e.g. drug induced structural variations) as well as intermolecular interactions in solution and at membrane surface (e.g. diffusion and clustering of membrane proteins). Combination of AFM with electrochemistry will allow us to drive and map electrochemical reactions at high spatial resolution. The scanning electrochemical microscope (SECM) is nowadays an established technique, but in the future, the development of AFM tips sensitive to other electrochemical processes is expected to enlarge the field of electrochemical signal retrieval at high spatial resolution and under controlled load (e.g. mapping ion channel distribution) [283].

8. Conclusions

In this review we have tried to provide an overview on the continuously growing field of AFM studies on the sample of biological interest. The field is too large for this paper to be exhaustive in reviewing all the various works which have been done on biosamples. Therefore, we have decided to focus our efforts on transmitting the feeling of how this technique can be exploited by researchers engaged in biophysical problems and how this technique can provide researchers with new information otherwise inaccessible by other techniques. Finally, we would like to apologize to all those whose work we have missed during the writing of this review.

Acknowledgment

This work has been partially supported by MUIR FIRB Nomade.

References

[1] Binnig G, Quate C F and Gerber C 1986 Atomic force microscope *Phys. Rev. Lett.* **56** 930–3
[2] Binnig G, Rohrer H, Gerber C and Weibel E 1982 Surface studies by scanning tunneling microscopy *Phys. Rev. Lett.* **49** 57–61

[3] Marti O, Elings V, Haugan M, Bracker C E, Schneir J, Drake B, Gould S A, Gurley J, Hellemans L and Shaw K 1988 Scanning probe microscopy of biological samples and other surfaces *J. Microsc.* **1521** 803–9
[4] Engel A 1991 Biological applications of scanning probe microscopes *Ann. Rev. Biophys. Chem.* **20** 79–108
[5] Radmacher M, Tillmann R W, Fritz M and Gaub H E 1992 From molecules to cells: imaging soft samples with the atomic force microscope *Science* **257** 1900–5
[6] Lindsay S M 1994 Biological scanning probe microscopy comes of age *Biophys. J.* **67** 2134–5
[7] Bustamante C and Keller D 1995 Scanning force microscopy in biology *Phys. Today* December 32–8
[8] Shao Z and Yang J 1995 Progress in high resolution atomic force microscopy in biology, *Q. Rev. Biophys.* **28** 195–251
[9] Shao Z, Yang J and Somlyo A P 1995 Biological atomic force microscopy: from microns to nanometers and beyond *Ann. Rev. Cell. Dev. Biol.* **11** 241–65
[10] Shao Z, Mou J, Czajkowsky D M, Yang J and Yuan J-Y 1996 Biological atomic force microscopy: what is achieved and what is needed *Adv. Phys.* **45** 1–86
[11] Drake B, Prater C B, Weisenhorn A L, Gould S A, Albrecht T R, Quate C F, Cannell D S, Hansma H G and Hansma P K 1989 Imaging crystals, polymers, and processes in water with the atomic force microscope, *Science* **243** 1586–9
[12] Bustamante C, Rivetti C and Keller D J 1997 Scanning force microscopy under aqueous solutions *Curr. Opin. Struct. Biol.* **7** 709–16
[13] Sarid D 1994 *Scanning Force Microscopy* 2nd edn (New York: Oxford University Press)
[14] Colton R J, Engel A, Frommer J E, Gaub H, Gewirth A A, Guckenberger A, Rabe J, Heckl W M and Parkinson B (ed) 1998 *Procedures in Scanning Probe Microscopy* (New York: Wiley)
[15] Giessibl F J 2003 Advances in atomic force microscopy *Rev. Mod. Phys.* **75** 949–83
[16] Meyer G and Amer N M 1988 Novel optical approach to atomic force microscopy *Appl. Phys. Lett.* **53** 1045–7
[17] Albrecht T R, Akamine S, Carver T E and Quate C F 1990 Microfabrication of cantilever styli for the atomic force microscope *J. Vac. Sci. Technol.* A **8** 3386–96
[18] Akamine S, Barrett R C and Quate C F 1990 Improved atomic force microscopy images using cantilevers with sharp tips *Appl. Phys. Lett.* **57** 316–8
[19] Wolter O, Bayer T and Greschner J 1991 Micromachined silicon sensors for scanning force microscopy *J. Vac. Sci. Technol.* A **9** 1353–7
[20] Dai H, Hafner J H and Lieber C M 1996 Nanotubes as nanoprobes in scanning probe microscopy *Nature* **384** 147–51
[21] Hafner J H, Cheung C-L, Woolley A T and Lieber C M 2001 Structural and functional imaging with carbon nanotube AFM probes *Prog. Biophys. Mol. Biol.* **77** 73–110
[22] Wong S S, Harper J D, Lansbury P T and Lieber C M 1998 Carbon nanotube tips: high-resolution probes for imaging biological systems *J. Am. Chem. Soc.* **120** 603–4
[23] Wong S S, Joselevich E, Woolley A T, Cheung C-L and Liber C M 1998 Covalently functionalized nanotubes as nanometer-sized probes in chemistry and biology *Nature* **394** 52–5
[24] Grigg D A, Russell P E and Griffith J E 1992 Tip–sample forces in scanning probe microscopy in air and vacuum *J. Vac. Sci. Technol.* A **10** 680–3
[25] Putman C A, van der Werf K O, de Grooth B G, van Hulst N F, Greve J and Hansma P K 1992 A new imaging mode in atomic force microscopy based on error signal *SPIE Scanning Probe Microsc.* **1693** 198–204
[26] Mate C M, McClelland M, Erlandsson R and Chiang S 1987 Atomic-scale friction of a tungsten tip on a graphite surface *Phys. Rev. Lett.* **59** 1942–5
[27] Frisbie C D, Rozsnyai L F, Noy A, Wrighton M S and Lieber C M 1994 Functional group imaging by chemical force microscopy *Science* **265** 2071–4
[28] Zhong Q, Inniss D, Kjoller K and Elings V B 1993 Fractured polymer/silica fiber surface studied by tapping mode atomic force microscope *Surf. Sci. Lett.* **290** L688–92
[29] Tamayo J and Garcia R 1996 Deformation, contact time, and phase-contrast in tapping mode scanning force microscopy *Langmuir* **12** 4430–5
[30] San Paulo A and Garcia R 2000 High-resolution imaging of antibodies by tapping-mode atomic force microscopy: attractive and repulsive tip–sample interaction regimes *Biophys. J.* **78** 1599–605
[31] Revenko I and Proksch R 2000 Magnetic and acoustic tapping mode microscopy of liquid phase phospholipid bilayers and DNA molecules *J. Appl. Phys.* **87** 526–33
[32] Han W, Lindsay S M and Jing T 1996 A magnetically driven oscillating probe microscope for operation in liquids *Appl. Phys. Lett.* **69** 4111–3
[33] Magonov S N, Elings V and Whangbo M-H 1997 Phase imaging and stiffness in tapping mode AFM *Surf. Sci.* **375** L385–91
[34] Cleveland J P, Anczykowski B, Schmid A E and Elings V B 1998 Energy-dissipation in tapping-mode atomic-force microscopy *Appl. Phys. Lett.* **72** 2613–5
[35] Tamayo J and Garcia R 1997 Effects of elastic and inelastic interactions on phase-contrast images in tapping-mode scanning force microscopy *Appl. Phys. Lett.* **71** 2394–6
[36] Hansma P K *et al* 1994 Tapping mode atomic force microscopy in liquids *Appl. Phys. Lett.* **64** 1738–40
[37] Putman C A J, van der Werf K O, de Grooth B G, van Hulst N F and Greve J 1994 Tapping mode atomic force microscopy in liquid *Appl. Phys. Lett.* **64** 2454–6
[38] Möller C, Allen M, Elings V, Engel A and Müller D J 1999 Tapping-mode atomic force microscopy produces faithful high-resolution images of protein surfaces *Biophys. J.* **77** 1150–8
[39] Stark M, Möller C, Müller D J and Guckenberger R 2001 From images to interactions: high-resolution phase imaging in tapping-mode atomic force microscopy *Biophys. J.* **80** 3009–18
[40] Tamayo J, Humphris A D L and Miles M J 2000 Piconewton regime dynamic force microscopy in liquid *Appl. Phys. Lett.* **77** 582–4
[41] Tamayo J, Humphris A D L, Owen R J and Miles M J 2001 High-Q dynamic force microscopy in liquid and its application to living cells *Biophys. J.* **81** 526–37
[42] Ohnesorge F and Binnig G 1993 True atomic resolution by atomic force microscopy through repulsive and attractive forces *Science* **260** 1451–6
[43] Müller D J, Fotiadis D, Scheuring S, Muller S A and Engel A 1999 Electrostatically balanced subnanometer imaging of biological specimens by atomic force microscope *Biophys J.* **76** 1101–11
[44] Uchihashi T *et al* 2000 Carbon-nanotube tip for highly-reproducible imaging of deoxyribonucleic acid helical turns by noncontact atomic force microscopy *Japan. J. Appl. Phys.* **39** L887–9
[45] Mou J, Czajkowsky D M, Yiyi Z and Shao Z 1995 High-resolution atomic-force microscopy of DNA: the pitch of the double helix *FEBS Lett.* **371** 279–82
[46] Wagner P 1998 Immobilization strategies for biological scanning probe microscopy *FEBS Lett.* **430** 112–5
[47] Thomson N H, Kasas S, Smith B, Hansma H G and Hansma P K 1996 Reversible binding of DNA to mica for AFM imaging *Langmuir* **12** 5905–8
[48] Hansma H G and Laney D E 1996 DNA binding to mica correlates with cationic radius: assay by atomic force microscopy *Biophys. J.* **70** 1933–9
[49] Pastre D, Pietrement O, Fusil P, Landousy F, Jeusset J, David M O, Hamon C, Le Cam E and Zozime A 2003 Adsorption of DNA to mica mediated by divalent

counterions: a theoretical and experimental study *Biophys. J.* **85** 2507–18
[50] Lyubchenko Y L and Shlyakhtenko L S 1997 Visualization of supercoiled DNA with atomic force microscopy *in situ* *Proc. Natl Acad. Sci. USA* **94** 496–501
[51] Weisenhorn A L, Egger M, Ohnesorge F, Gould S A C, Heyn S-P, Sinsheimer L, Gaub H E, Hansma H G and Hansma P K 1991 Molecular-resolution images of Langmuir–Blodgett films and DNA by atomic force microscopy *Langmuir* **7** 8–12
[52] Samori B, Muzzalupo I and Zuccheri G 1996 Deposition of supercoiled DNA on mica for scanning force microscopy imaging *Scanning Microsc.* **10** 953–60
[53] Okada T and Tanigawa M 1998 Atomic force microscopy of supercoiled DNA structure on mica *Anal. Chim. Acta* **365** 19–25
[54] Rivetti C, Guthold M and Bustamante C 1996 Scanning force microscopy of DNA deposited onto mica: equilibration *versus* kinetic trapping studied by statistical polymer chain analysis *J. Mol. Biol.* **264** 919–32
[55] Tanigawa M and Okada T 1998 Atomic force microscopy of supercoiled DNA structure on mica *Anal. Chim. Acta* **365** 19–25
[56] Lyubchenko Y L, Gall A A, Shlyakhtenko L S, Harrington R E, Jacobs B L, Oden P I and Lindsay S M 1992 *J. Biomol. Struct. Dyn.* **10** 589–606
[57] Bustamante C, Erie D A and Keller D 1994 Biochemical and structural applications of scanning force microscopy *Curr. Opin. Struct. Biol.* **3** 750–60
[58] Chen L, Cheung C L, Ashby P D and Lieber C M 2004 Single-walled carbon nanotube AFM probes: optimal imaging resolution of nanoclusters and biomolecules in ambient and fluid environment *Nano Lett.* **4** 1725–31
[59] Yang J and Shao Z 1993 Effect of probe force on the resolution of atomic force microscopy of DNA *Ultramicroscopy* **50** 157–70
[60] Moreno-Herrero F, Colchero J and Baró A M 2003 DNA height in scanning force microscopy *Ultramicroscopy* **96** 167–74
[61] Rippe K, Mucke N and Langowski J 1997 Superhelix dimensions of a 1868 base pair plasmid determined by scanning force microscopy in air and in aqueous solution *Nucleic Acids Res.* **25** 1736–44
[62] Pope L H, Davies M C, Laughton C A, Roberts C J, Tendler S J B and Williams P M 1999 Intercalation-induced changes in DNA supercoiling observed in real-time by atomic force microscopy *Anal. Chim. Acta* **400** 27–32
[63] Cherny D I, Fourcade A, Svinarchuk F, Nielsen P E, Malvy C and Delain E 1998 Analysis of various sequence-specific triplexes by electron and atomic force microscopies *Biophys. J.* **74** 1015–23
[64] Marsh T C, Vesenka J and Henderson E 1995 A new DNA nanostructure, the G-wire, imaged by scanning probe microscopy *Nucleic Acids Res.* **23** 696–700
[65] Murakami M, Hirokawa H and Hayata I 2000 Analysis of radiation damage of DNA by atomic force microscopy in comparison with agarose gel electrophoresis studies *J. Biochem. Biophys. Methods* **44** 31–40
[66] Murakami M, Minamihisamatsu M, Sato K and Hayata I 2001 Structural analysis of heavy ion radiation-induced chromosome aberrations by atomic force microscopy *J. Biochem. Biophys. Methods* **48** 293–301
[67] Lysetska M, Knoll A, Boehringer D, Hey T, Krauss G and Krausch G 2002 UV light-damaged DNA and its interaction with human replication protein A: an atomic force microscopy study *Nucleic Acids Res.* **30** 2686–91
[68] Pang D, Popescu G, Rodgers J, Berman B L and Dritschilo A 1996 Atomic force microscopy investigation of radiation-induced DNA double strand breaks *Scanning Microsc.* **10** 1105–10
[69] Berge T, Jenkins N S, Hopkirk R B, Waring M J, Edwardson J M and Henderson R M 2002 Structural perturbations in DNA caused by bis-intercalation of ditercalinium visualised by atomic force microscopy *Nucleic Acids Res.* **30** 2980–6
[70] Laughton C A, Tendler S J B, Williams P M, Roberts C J, Davies M C and Pope L H 1999 Intercalation-induced changes in DNA supercoiling observed in real-time by atomic force microscopy *Anal. Chim. Acta* **400** 27–32
[71] Pope L H, Davies M C, Laughton C A, Roberts C J, Tendler S J B and Williams P M 2000 Atomic force microscopy studies of intercalation-induced changes in plasmid DNA tertiary structure *J. Microsc.* **199** 68–78
[72] Klinov D V, Lagutina I V, Prokhorov V V, Neretina T, Khil P P, Lebedev Y B, Cherny D I, Demin V V and Sverdlov E D 1998 High resolution mapping DNAs by R-loop atomic force microscopy *Nucleic Acids Res.* **26** 4603–10
[73] Rippe K, Guthold M, von Hippel P H and Bustamante C 1997 Transcriptional activation via DNA-looping: visualization of intermediates in the activation pathway of *E. coli* RNA polymerase x sigma 54 holoenzyme by scanning force microscopy *J. Mol. Biol.* **270** 125–38
[74] van Noort J, Orsini F, Eker A, Wyman C, de Grooth B and Greve J 1999 DNA bending by photolyase in specific and non-specific complexes studied by atomic force microscopy *Nucleic Acids Res.* **27** 3875–80
[75] Valle M, Valpuesta J M, Carrascosa J L, Tamayo J and Garcia R 1996 The interaction of DNA with bacteriophage phi 29 connector: a study by AFM and TEM *J. Struct. Biol.* **116** 390–8
[76] Garcia R A, Bustamante C J and Reich N O 1996 Sequence-specific recognition by cytosine C^5 and adenine N^6 DNA methyltransferases requires different deformations of DNA *Proc. Natl Acad. Sci. USA* **93** 7618–22
[77] Palecek E, Vlk D, Stankova V, Brazda V, Vojtesek B, Hupp T R, Schaper A and Jovin T M 1997 Tumor suppressor protein p53 binds preferentially to supercolied DNA *Oncogene* **15** 2201–9
[78] Guthold M, Zhu X, Rivetti C, Yang G, Thomson N H, Kasas S, Hansma H G, Smith B, Hansma P K and Bustamante C 1999 Direct observation of one-dimensional diffusion and transcription by *Escherichia coli* RNA polymerase *Biophys. J.* **77** 2284–94
[79] Jiao Y, Cherny D I, Heim G, Jovin T M and Schäffer T E 2001 Dynamic interactions of p53 with DNA in solution by time-lapse atomic force microscopy *J. Mol. Biol.* **314** 233–43
[80] Jett S D, Cherny D I, Subramaniam V and Jovin T M 2000 Scanning force microscopy of the complexes of p53 core domain with supercoiled DNA *J. Mol. Biol.* **299** 585–92
[81] Pietrasanta L I, Thrower D, Hsieh W, Rao S, Stemmann O, Lechner J, Carbon J and Hansma H 1999 Probing the *Saccharomyces cerevisiae* centromeric DNA (CEN DNA)-binding factor 3 (CBF3) kinetochore complex by using atomic force microscopy *Proc. Natl Acad. Sci. USA* **96** 3757–62
[82] Lin Z, Wang C, Feng X, Liu M, Li J and Bai C 1998 The observation of the local ordering characteristics of spermidine-condensed DNA: atomic force microscopy and polarizing microscopy studies *Nucleic Acids Res.* **26** 3228–34
[83] Bustamante C, Zuccheri G, Leuba S H, Yang G and Samorì B 1997 Visualization and analysis of chromatin by scanning force microscopy *Methods* **12** 73–83
[84] Leuba S H, Bustamante C, van Holde K and Zlatanova J 1998 Linker histone tails and N-tails of histone H3 are redundant: scanning force microscopy studies of reconstituted fibers *Biophys. J.* **74** 2830–9
[85] de Grauw C J, Avogadro A, van den Heuvel D J, vd Werf K O, Otto C, Kraan Y, van Hulst N F and Greve J 1998 Chromatin structure in bands and interbands of polytene chromosomes imaged by atomic force microscopy *J. Struct. Biol.* **121** 2–8

[86] Wang H, Bash R, Yodh J G, Hager G L, Lohr D and Lindsay S M 2002 Glutaraldehyde modified mica: a new surface for atomic force microscopy of chromatin *Biophys. J.* **83** 3619–25
[87] Hoh J H, Lal R, John S A, Revel J P and Arnsdorf M F 1991 Atomic force microscopy and dissection of gap junctions *Science* **253** 1405–8
[88] Arakawa H, Umemura K and Ikai A 1992 Protein images obtained by ATM, AFM and TEM *Nature* **358** 171–3
[89] Müller D J, Amrein M and Engel A 1997 Adsorption of biological molecules to a solid support for scanning probe microscopy *J. Struct. Biol.* **119** 172–88
[90] Fotiadis D, Scheuring S, Müller S A, Engel A and Müller D J 2002 Imaging and manipulation of biological structures with the AFM *Micron* **33** 385–97
[91] Mou J, Czajkowsky D M, Sheng S, Ho R and Shao Z 1996 High resolution surface structure of *E. coli* GroES oligomer by atomic force microscopy *FEBS Lett.* **381** 161–4
[92] Cheung C-L, Hafner J H and Lieber C M 2000 Carbon nanotube atomic force microscopy tips: direct growth by chemical vapor deposition and applications to high-resolution imaging *Proc. Natl Acad. Sci. USA* **97** 3809–13
[93] Zhang Y, Sheng S J and Shao Z 1996 Imaging biological structures with the cryo atomic force microscope *Biophys. J.* **71** 2168–76
[94] Hafner J H, Cheung C-L and Lieber C M 1999 Growth of nanotubes for probe microscopy tips *Nature* **398** 761–2
[95] Alessandrini A, Gerunda M, Facci P, Schnyder B and Koetz R 2003 Tuning molecular orientation in protein films *Surf. Sci.* **542** 64–71
[96] Wadu-Mesthrige K, Amro N A and Liu G Y 2000 Immobilization of proteins on self-assembled monolayers *Scanning* **22** 380–8
[97] Müller D J and Engel A 1999 Voltage and pH-induced channel closure of Porin OmpF visualized by atomic force microscopy *J. Mol. Biol.* **285** 1347–51
[98] Schabert F A, Henn C and Engel A 1995 Native *Escherichia coli* OmpF porin surface probed by atomic force microscopy *Science* **268** 92–4
[99] Heymann J B, Müller D J, Landau E, Rosenbusch J, Pebay-Peroulla E, Büldt G and Engel A 1999 Charting the surfaces of purple membrane *J. Struct. Biol.* **128** 243–9
[100] Müller D J, Baumeister W and Engel A 1996 Conformational change of the hexagonally packed intermediate layer of *Deinococcus radiodurans* monitored by atomic force microscopy *J. Bacteriol.* **178** 3025–30
[101] Seelert H, Poetsch A, Dencher N A, Engel A, Stahlberg H and Müller D J 2000 Proton powered turbine of a plant motor *Nature* **405** 418–9
[102] Müller D J, Engel A, Carrascosa J and Veléz M 1997 The bacteriophage ϕ 29 head–tail connector imaged at high resolution with atomic force microscopy in buffer solution *EMBO J.* **16** 101–7
[103] Walz T, Tittmann P, Fuchs K H, Müller D J, Smith B L, Agre P, Gross H and Engel A 1996 Surface topographies at subnanometer-resolution reveal asymmetry and sidedness of aquaporin-1 *J. Mol. Biol.* **264** 907–18
[104] Scheuring S, Ringler P, Borgina M, Stahlberg H, Müller D J, Agre P and Engel A 1999 High resolution topographs of the *E. coli* waterchannel acquporin Z *EMBO J.* **18** 4981–7
[105] Fotiadis D, Hasler L, Müller D J, Stahlberg H, Kistler J and Engel A 2000 Surface tongue-and-groove contours on lens MIP facilitate cell-to-cell adherence *J. Mol. Biol.* **300** 779–89
[106] Müller D J, Hand G M, Engel A and Sosinsky G E 2002 Conformational changes in surface structures of isolated connexin 26 gap junctions *EMBO J.* **21** 3598–607
[107] Müller D J, Engel A, Matthey U, Meier T, Dimroth P and Suda K 2003 Observing membrane protein diffusion at subnanometer resolution *J. Mol. Biol.* **327** 925–30
[108] Schillers H, Danker T, Schnittler H J and Oberleithner H 2000 Plasma membrane plasticity of *Xenopus laevis* oocyte imaged with atomic force microscopy *Cell Physiol. Biochem.* **10** 99–107
[109] Danker T and Oberleithner H 2000 Nuclear pore function viewed with atomic force microscopy *Pflugers Arch.* **439** 671–81
[110] Schillers H, Shanin V, Albermann L, Schafer C and Oberleithner H 2004 Imaging CFTR: a tail-to-tail dimer with a central pore *Cell Physiol. Biochem.* **14** 1–10
[111] Dufrêne Y F and Lee G U 2000 Advances in the characterization of supported lipid films with the atomic force microscope *Biochim. Biophys. Acta* **1509** 14–41
[112] Balashev K, Jensen T R, Kjaer K and Bjørnholm T 2001 Novel methods for studying lipids and lipases and their mutual interaction at interfaces: Part I. Atomic force microscopy *Biochimie* **83** 387–97
[113] Jass J, Tjärnhage T and Puu G 2000 From liposomes to supported, planar bilayer structures on hydrophilic and hydrophobic surfaces: an atomic force microscopy study *Biophys. J.* **79** 3153–63
[114] Leonenko Z V, Carnini A and Cramb D T 2000 Supported planar bilayer formation by vesicle fusion: the interaction of phospholipid vesicles with surfaces and the effect of gramicidin on bilayer properties using atomic force microscopy *Biochim. Biophys. Acta* **1509** 131–47
[115] Zasadzinski J A N, Helm C A, Longo L M, Weisenhorn A L, Gould S A C and Hansma P K 1991 Atomic force microscopy of hydrated phosphatidylethanolamine bilayers, *Biophys. J.* **59** 755–60
[116] Hui S W, Viswanathan R, Zasadzinski J A and Israelachvili J 1995 The structure and stability of phospholipid bilayers by atomic force microscopy *Biophys. J.* **68** 171–8
[117] Muscatello U, Valdrè G and Valdrè U 1996 Atomic force microscopy observations of acyl chains in phospholipids *J. Microscopy* **182** 200–7
[118] Zhai X and Kleijn J M 1997 Molecular structure of dipalmitoylphosphatidylcholine Langmuir–Blodgett monolayers studied by atomic force microscopy *Thin Solid Film* **304** 327–32
[119] Mou J, Yang J, Huang C and Shao Z 1994 Alcohol induces interdigitated domains in unilamellar phosphatidylcholine bilayers *Biochemistry* **33** 9981–5
[120] Giocondi M C, Pacheco L, Millhiet P E and Le Grimellec C 2001 Temperature dependence of the topology of supported dimirystoil-distearoyl phosphatidylcholine bilayers *Ultramicroscopy* **86** 151–7
[121] Fang Y and Yang J 1997 The growth of bilayer defects and the induction of interdigitated domains in the lipid-loss process of supported phospholipid bilayers *Biochim. Biophys. Acta* **1324** 309–19
[122] Kaasgaard T, Leidy C, Crowe J H, Mouritsen O G and Jørgensen K 2003 Temperature-controlled structure and kinetics of ripple phases in one- and two-component supported lipid bilayers *Biophys. J.* **85** 350–60
[123] Yang X M, Xiao D, Xiao S J and Wei Y 1994 Domain-structures of phospholipid monolayer Langmuir–Blodgett films determined by atomic force microscopy *Appl. Phys.* A **59** 139–43
[124] Henderson R M, Edwardson J M, Geisse N A and Saslowsky D E 2004 Lipid rafts: feeling is believing *News Physiol. Sci.* **19** 39–43
[125] Rinia H A, Snell M M E, van der Eerden J P and de Kruijff B 2001 Visualizing detergent resistant domains in model membranes with atomic force microscopy *FEBS Lett.* **501** 92–6
[126] Saslowski D E, Lawrence J, Ren X, Brown D A, Henderson R M and Edwardson J M 2002 Placental alkaline phosphatase is efficiently targeted rafts in supported lipid bilayers *J. Biol. Chem.* **277** 26966–70

[127] Xiao X, Hu J, Charych D H and Salmeron M 1996 Chain length dependence of the frictional properties of alkylsilane molecules self-assembled on mica studied by atomic force microscopy *Langmuir* **12** 235–7
[128] Dufrêne Y F, Barger W R, Green J-B D and Lee G U 1997 Nanometer-scale surface properties of mixed phospholipid monolayers and bilayers *Langmuir* **13** 4779–84
[129] Mou J, Czajkowsky D M and Shao Z 1996 Gramicidin A aggregation in supported gel state phosphatidylcholine bilayers *Biochemistry* **35** 3222–6
[130] Rinia H A, Boots J-W P, Rijkers D T S, Kik R A, Snel M M E, Demel R A, Killian J A, van der Eerden J P J M and de Kruijff B 2002 Domain formation in phosphatidylcholine bilayers containing transmembrane peptides: specific effects of flanking residues *Biochemistry* **41** 2814–24
[131] Deleu M, Paquot M, Jacques P, Thonart P, Adriaensen Y and Dufrêne Y F 1999 Nanometer scale organization of mixed surfactin/phosphatidylcholine monolayers *Biophys. J.* **17** 2304–10
[132] Boussad S, Dziri L, Arechabaleta R, Tao N J and Leblanc R M 1998 Electron-transfer properties of cytochrome c Langmuir–Blodgett films and interactions of cytochrome c with lipids *Langmuir* **14** 6215–9
[133] Reviakine I, Bergsma-Schutter W, Mazeres-Dubut C, Govorukhina N and Brisson A 2000 Surface topography of the p3 and p6 annexin V crystal forms determined by atomic force microscopy *J. Struct. Biol.* **131** 234–9
[134] Hoh J H and Hansma P K 1992 Atomic force microscopy for high resolution imaging in cell biology *Trends Cell Biol.* **2** 208–13
[135] Henderson E R 1994 Imaging living cells by atomic force microscopy *Prog. Surf. Sci.* **46** 39–60
[136] Nagao E and Dvorak J A 1998 An integrated approach to the study of living cells by atomic force microscopy *J. Microsc.* **191** 8–19 (Riferimento sulle imaging conditions di cellule)
[137] Dvorak J A 2003 The application of atomic force microscopy to the study of living vertebrate cells in culture *Methods* **29** 86–96
[138] Putman C A J, van der Werf K O, de Grooth B G, van Hulst N F and Greve J 1994 Viscoelasticity of living cells allows high resolution imaging by tapping mode atomic force microscopy *Biophys. J.* **67** 1749–53
[139] Hansma H G, Kim K J, Laney D E, Garcia R A, Argaman M, Allen M J and Parson S M 1997 Properties of biomolecules measured from atomic force microscope images: a review *J. Struct. Biol.* **119** 99–108
[140] Nagao E and Dvorak J A 1999 Phase imaging by atomic force microscopy: analysis of living homoiothermic vertebrate cells *Biophys. J.* **76** 3289–97
[141] Henderson E, Haydon P G and Sakaguchi D S 1992 Actin filament dynamics in living glial cells imaged by atomic force microscopy *Science* **257** 1944–6
[142] Hofmann U G, Rotsch C, Parak W J and Radmacher M 1997 Investigating the cytoskeleton of chicken cardiocytes with the atomic force microscope *J. Struct. Biol.* **119** 84–91
[143] Rotsch C, Jacobson K and Radmacher M 1997 Investigating living cells with the atomic force microscope *Scanning Microsc.* **11** 1–8
[144] Rotsch C, Jacobson K and Radmacher M 1999 The dynamics of active and stable edges in motile fibroblasts investigated by atomic force microscopy *Proc. Natl Acad. Sci. USA* **96** 921–6
[145] Rotsch C and Radmacher M 2000 Drug-induced changes of cytoskeletal structure and mechanics in fibroblasts: an atomic force microscopy study *Biophys. J.* **78** 520–35
[146] Haga H, Sasaki S, Kawabata K, Ito E, Ushiki T and Sambongi T 2000 Elasticity mapping of living fibroblasts by AFM and immunofluorescence observation of the cytoskeleton *Ultramicroscopy* **82** 253–8
[147] Oberleithner H, Giebisch G and Geibel J 1993 Imaging the lamellipodium of migrating epithelial cells *in vivo* by atomic force microscopy *Pflugers Arch.* **425** 506–10
[148] Matzke R, Jacobson K and Radmacher M 2001 Direct, high-resolution measurement of furrow stiffening during division of adherent cells *Nat. Cell Biol.* **3** 607–10
[149] Schoenenberger C A and Hoh J H 1994 Slow cellular dynamics in MDCK and R5 cells monitored by time-lapse atomic force microscopy *Biophys. J.* **67** 929–36
[150] Charras G T and Horton M A 2002 Single cell mechanotransduction and its modulation analysed by atomic force microscope indentation *Biophys. J.* **82** 2970–81
[151] Schneider S W, Yano Y, Sumpio B E, Jena B P, Geibel J P, Gekle M and Oberleithner H 1997 Rapid aldosterone-induced cell volume increase of endothelial cells measured by the atomic force microscope *Cell. Biol. Int.* **21** 759–68
[152] Dufrêne Y F 2004 Refining our perception of bacterial surfaces with the atomic force microscope *J. Bacteriol.* **186** 3283–5
[153] Dufrêne Y F 2001 Application of atomic force microscopy to microbial surfaces: from reconstituted cell surface layers to living cells *Micron* **32** 153–65
[154] Kasas S and Ikai A 1995 A method for anchoring round shaped cells for atomic force microscope imaging *Biophys. J.* **68** 1678–80
[155] Dufrêne Y F, Boonaert C J P, Gerin P A, Asther M and Rouxhet P G 1999 Direct probing of the surface ultrastructure and molecular interactions of dormant and germinating spores of *Phanerochaete chrysosporium* *J. Bacteriol.* **181** 5350–4
[156] Ahimou F, Touhami A and Dufrêne Y F 2003 Real-time imaging of the surface topography of living yeast cells by atomic force microscopy *Yeast* **20** 25–30
[157] Cappella B, Baschieri P, Frediani C, Miccoli P and Ascoli C 1997 Force–distance curves by AFM *IEEE Eng. Med. Biol.* **16** 58–65
[158] Cappella B and Dietler G 1999 Force–distance curves by atomic force microscopy *Surf. Sci. Rep.* **34** 1–104
[159] Thomas R C, Houston J E, Crooks R M, Kim T and Michalske T A 1995 Probing adhesion forces at the molecular scale *J. Am. Chem. Soc.* **117** 3830–4
[160] Nakagawa T, Ogawa K and Kurumizawa T 1994 Atomic force microscope for chemical sensing *J. Vac. Sci. Technol.* B **12** 2215–8
[161] Nakagawa T, Ogawa K, Kurumizawa T and Ozaki S 1993 Discriminating molecular length of chemically adsorbed molecules using an atomic force microscope having a tip covered with sensor molecules (an atomic force microscope having chemical sensing function) *Japan. J. Appl. Phys.* **32** L294–6
[162] Sinniah S K, Steel A B, Miller C J and Reutt-Robey J E 1996 Solvent exclusion and chemical contrast in scanning force microscopy *J. Am. Chem. Soc.* **118** 8925–31
[163] Noy A, Frisbie C D, Rozsnyai L F, Wrighton M S and Lieber C M 1995 Chemical force microscopy: exploiting chemically-modified tips to quantify adhesion, friction, and functional group distributions in molecular assemblies *J. Am. Chem. Soc.* **117** 7943–51
[164] Heinz W F and Hoh J H 1999 Spatially resolved force spectroscopy of biological surfaces using the atomic force microscope *Trends Biotechnol.* **17** 143–50
[165] Sader J E and White L 1993 Theoretical analysis of the static deflection of plates for atomic force microscope applications *J. Appl. Phys.* **74** 1–9
[166] Sader J E 1995 Parallel beam approximation for V-shaped atomic force microscope cantilevers *Rev. Sci. Instrum.* **66** 4583–7
[167] Chen G Y, Warmack R J, Huang A and Thundat T 1995 Harmonic response of near-contact scanning force microscopy *J. Appl. Phys.* **78** 1465–9

[168] Chen G Y, Warmack RJ, Thundat T, Allison D P and Huang A 1994 Resonance response of scanning force microscopy cantilevers, *Rev. Sci. Instrum.* **65** 2532–7
[169] Senden T J and Ducker W A 1994 Experimental determination of spring constants in atomic force microscopy *Langmuir* **10** 1003–4
[170] Sader J E, Larson I, Mulvaney P and White L R 1995 Method for calibration of atomic force microscope cantilevers, *Rev. Sci. Instrum.* **66** 3789–98
[171] Hutter J L and Bechhoefer J 1993 Calibration of atomic-force microscope tips *Rev. Sci. Instrum.* **64** 1868–73
[172] Cleveland J E, Manne S, Bocek D and Hansma P K 1993 A non destructive method for determining the spring constant of cantilevers for scanning force microscopy *Rev. Sci. Instrum.* **64** 403–5
[173] Radmacher M, Cleveland J P, Fritz M, Hansma H G and Hansma P K 1994 Mapping interaction forces with the atomic force microscope *Biophys. J* **66** 2159–65
[174] Cleveland J P, Radmacher M and Hansma P K 1994 Atomic scale force mapping with the atomic force microscope *NATO Advanced Research Workshop* pp 543–9
[175] Green N H, Allen S, Davies M C, Roberts C J, Tendler S J B and Williams P M 2002 Force sensing and mapping by atomic force microscopy *Trends Anal. Chem.* **21** 64–74
[176] Willemsen O H, Snel M E, Cambi A, Greve J, De Grooth B G and Figdor C G 2000 Biomolecular interactions measured by atomic force microscopy *Biophys. J.* **79** 3267–81
[177] Tao N J, Lindsay S M and Lees S 1992 Measuring the microelastic properties of biological material *Biophys. J.* **63** 1165–9
[178] Costa K D and Yin F C P 1999 Analysis of indentation: implications for measuring mechanical properties with atomic force microscopy *J. Biomech. Eng.* **121** 462–71
[179] Radmacher M, Fritz M, Cleveland J P, Walters D A and Hansma P K 1994 Imaging adhesion forces and elasticity of lysozyme adsorbed on mica with the atomic force microscope *Langmuir* **10** 3809–14
[180] Vinckier A and Semenza G 1998 Measuring elasticity of biological materials by atomic force microscopy *FEBS Lett* **430** 12–6
[181] Hertz H 1881 Über den kontakt elastischer körper *J. Reine Angew. Math.* **92** 156
[182] Sneddon I N 1965 The relaxation between load and penetration in the axisymmetric Boussinesq problem for a punch of arbitrary profile *Int. J. Eng. Sci.* **3** 47–57
[183] Radmacher M, Tillman R W and Gaub H E 1993 Imaging viscoelasticity by force modulation with the atomic force microscope *Biophys. J.* **64** 735–42
[184] Alcaraz J, Buscemi L, Grabulosa M, Trepat X, Fabry B, Farré R and Navajas D 2003 Microrheology of human lung epithelial cells measured by atomic force microscopy *Biophys. J.* **84** 2071–9
[185] Mathur A B, Collinsworth A M, Reichert W M, Kraus W E and Truskey G A 2001 Endothelial, cardiac muscle and skeletal muscle exhibit different viscous and elastic properties as determined by atomic force microscopy *J. Biomech.* **34** 1545–53
[186] Mahaffy R E, Park S, Gerde E, Kas J and Shih C K 2004 Quantitative analysis of the viscoelastic properties of thin regions of fibroblasts using atomic force microscopy *Biophys. J.* **86** 1777–93
[187] A-Hassan E, Heinz W F, Antonik M D, D'Costa N P, Nageswaran S, Schoenenberger C-A and Hoh J H 1998 Relative microelastic mapping of living cells by atomic force microscopy *Biophys. J.* **74** 1564–78
[188] Wu H W, Kuhn T and Moy V T 1998 Mechanical properties of L929 cells measured by atomic force microscopy: effects of anticytoskeletal drugs and membrane crosslinking *Scanning* **20** 389–97
[189] Ikai A, Mitsui K, Tokouka H and Xu X M 1997 Mechanical measurements of a single protein molecule and human chromosome by the atomic force microscope *Mater. Sci. Eng.* C **4** 233–40
[190] Simon A, Cohen-Bouhacina T, Aime J P, Porte M C, Amedee J and Baquey C 2004 Heterogeneous cell mechanical properties: an atomic force microscopy study *Cell. Mol. Biol.* **50** 255–66
[191] Brown H G and Hoh J H 1997 Entropic exclusion by neurofilament sidearms: a mechanism for maintaining interfilament spacing *Biochemistry* **36** 15035–40
[192] Butt H J 1992 Measuring local surface-charge densities in electrolyte-solutions with a scanning force microscope *Biophys. J.* **63** 578–82
[193] Müller D J and Engel A 1997 The height of biomolecules measured with the atomic force microscope depends on electrostatic interactions *Biophys. J.* **73** 1633–44
[194] Shroff S G, Saner D R and Lal R 1995 Dynamic micromechanical properties of cultured rat atrial myocytes measured by atomic force microscopy *Am. J. Physiol.* **269** C286–92
[195] Walch M, Ziegler U and Groscurth P 2000 Effect of streptolysin O on the microelasticity of human platelets analyzed by atomic force microscopy *Ultramicroscopy* **82** 259–67
[196] Radmacher M 1997 Measuring the elastic properties of biological samples with the AFM *IEEE Eng. Med. Biol. Mag.* **16** 47–57
[197] Goldmann W H, Galneder R, Ludwig M, Xu W, Adamson E D, Wang N and Ezzell R M 1998 Differences in elasticity of vinculin-deficient F9 cells measured by magnetometry and atomic force microscopy *Exp. Cell. Res.* **239** 235–42
[198] Domke J, Parak W J, George M, Gaub H E and Radmacher M 1999 Mapping the mechanical pulse of single cardiomyocytes with the atomic force microscope *Eur. Biophys. J.* **28** 179–86
[199] Noy A, Vezednov D V and Lieber C M 1997 Chemical force microscopy *Ann. Rev. Mater. Sci.* **27** 381–421
[200] Hinterdorfer P, Baumgartner W, Gruber H J, Schilcher K and Schindler H 1996 Detection and localization of individual antibody–antigen recognition events by atomic force microscopy *Proc. Natl Acad. Sci.USA* **93** 3477–81
[201] Hinterdorfer P, Schilcher K, Baumgartner W, Gruber H J and Schindler H 1998 A mechanistic study of the dissociation of individual antibody–antigen pairs by atomic force microscopy *Nanobiology* **4** 39–50
[202] Haselgrübler Th, Amerstorfer A, Schindler H and Gruber H J 1995 Synthesis and application of a new poly(ethylene) glycol derivative for the crosslinking of amines with thiols *Bioconjugate Chem.* **6** 242–8
[203] Grandbois M, Beyer M, Rief M, Clausen-Schaumann H and Gaub H E 1999 How strong is a covalent bond? *Science* **283** 1727–30
[204] Merkel R, Nassoy P, Leung A, Ritchie K and Evans E 1999 Energy landscapes of receptor–ligand bonds explored with dynamic force spectroscopy *Nature* **397** 50–3
[205] Lee G U, Kidwell D A and Colton R J 1994 Sensing discrete streptavidin–biotin interactions with the atomic force microscopy *Langmuir* **10** 354–7
[206] Florin E L, Moy V T and Gaub H E 1994 Adhesion forces between individual ligand receptor pairs *Science* **264** 415–7
[207] Hinterdorfer P, Gruber H J, Schilcher K, Baumgartner W, Hasel-gruebler T and Schinler H 1995 Antibody–antigen unbinding forces measured by force microscopy using antibodies bound to AFM tips via a specially designed flexible crosslinker *Biophys. J.* **68** 139a (Abstr.)
[208] Stuart J K and Hlady V 1995 Effects of discrete protein–surface interactions in scanning force microscopy adhesion force measurements *Langmuir* **11** 1368–74
[209] Ros R, Schwesinger F, Anselmetti D, Kubon M, Schaefer R, Plückthun A and Tiefenauer L 1998 Antigen binding forces of individually addressed single-chain Fv antibody molecules *Proc. Natl Acad. Sci. USA* **95** 7402–5

[210] Dammer U, Hegner M, Anselmetti D, Wagner P, Dreier M, Huber W and Güntherodt H-J 1996 Specific antigen/antibody interactions measured by force microscopy *Biophys. J.* **70** 2437–41
[211] Allen S, Chen X, Davies J, Davies M C, Dawkes A C, Edwards J C, Roberts C J, Sefton J, Tendler S J B and Williams P M 1997 Spatial mapping of specific molecular recognition sites by atomic force microscopy *Biochemistry* **36** 7457–63
[212] Willemsen O H, Snel M M E, van der Werf K O, de Grooth B G, Greve J, Hinterdorfer P, Gruber H J, Schindler H, van Kooyk Y and Figdor C G 1998 Simultaneous height and adhesion imaging of antibody antigen interactions by atomic force microscopy *Biophys. J.* **75** 2220–8
[213] Lee G U, Chrisey L A and Colton R J 1994 Direct measurement of the forces between complementary strands of DNA *Science* **266** 771–3
[214] Strunz T, Oroszlan K, Schumkovitch I and Güntherodt H-J 1999 Dynamic force spectroscopy of single DNA molecules *Proc. Natl Acad. Sci. USA* **96** 11277–82
[215] Boland T and Ratner B D 1995 Direct measurement of hydrogen bonding in DNA nucleotide bases by atomic force microscopy *Proc. Natl Acad. Sci. USA* **92** 5297–301
[216] Noy A, Vezenov D V, Kayyem J F, Meade T J and Lieber C M 1997 Stretching and breaking duplex DNA by chemical force microscopy *Chem. Biol.* **4** 519–27
[217] Mazzola L T, Frank C W, Fodor S P A, Mosher C, Lartius R and Henderson E 1999 Discrimination of DNA hybridization using chemical force microscopy *Biophys. J.* **76** 2922–33
[218] Rief M, Clausen-Schaumann H and Gaub H E 1999 Sequence dependent mechanics of single DNA molecules *Nat. Struct. Biol.* **6** 346–9
[219] Bockelmann U, Essevaz-Roulet B and Heslot F 1997 Molecular stick-slip motion revealed by opening DNA with pico-Newton forces *Phys. Rev. Lett.* **79** 4489–92
[220] Lehenkari P P and Horton M A 1999 Single integrin molecule adhesion forces in intact cells measured by atomic force microscopy *Biochem. Biophys. Res. Commun.* **259** 645–50
[221] Grandbois M, Dettman W, Benoit M and Gaub H E 2000 Affinity imaging of red blood cells with an atomic force microscope *J. Hist. Cyt.* **48** 719–24
[222] van der Werf K O, Putman C A J, de Grooth B G and Greve J 1994 Adhesion force imaging in air and liquid by adhesion mode atomic force microscopy *Appl. Phys. Lett.* **65** 1195–7
[223] Ludwig M, Dettmann W and Gaub H E 1997 Atomic force microscope imaging contrast based on molecular recognition *Biophys. J.* **72** 445–8
[224] Willemsen O H, Snel M M E, Kuipers L, Figdor C G, Greve J and de Grooth B G 1999 A physical approach to reduce nonspecific adhesion in molecular recognition atomic force microscopy *Biophys. J.* **76** 716–24
[225] Yuan C, Chen A, Kolb P and Moy V T 2000 Energy landscape of streptavidin–biotin complexes measured by atomic force microscopy *Biochemistry* **39** 10219–23
[226] Evans E and Ritchie K 1997 Dynamic strength of molecular adhesion bonds *Biophys. J.* **72** 1541–55
[227] Schwesinger F, Ros R, Strunz T, Anselmetti D, Güntherodt H J, Honegger A, Jermutus L, Tiefenauer L and Plückthun A 2000 Unbinding forces of single antibody–antigen complexes correlate with their thermal dissociation rates *Proc. Natl Acad. Sci. USA* **97** 9972–7
[228] Strunz T, Oroszlan K, Schumkovitch I, Güntherodt H-J and Hegner M 2000 Model energy landscapes and the force-induced dissociation of ligand–receptor bonds *Biophys. J.* **79** 1206–12
[229] Baumgartner W, Hinterdorfer P, Ness W, Raab A, Vestweber D, Schindler H and Drenckhahn D 2000 Cadherin interaction probed by atomic force microscopy *Proc. Natl Acad. Sci. USA* **97** 4005–10
[230] Ludwig M, Dettmann W and Gaub H E 1997 Atomic force microscope imaging contrast based on molecular recognition *Biophys. J.* **72** 445–48
[231] Raab A, Han W, Badt D, Smith-Gill S J, Lindsay S M, Schindler H and Hinterdorfer P 1999 Antibody recognition imaging by force microscopy *Nat. Biotechnol.* **17** 901–5
[232] Samori B 1998 Stretching, tearing, and dissecting single molecules of DNA *Angew. Chem. Int. Ed.* **37** 2198–2200
[233] Clausen-Scaumann H, Rief M, Tolksdorf C and Gaub H E 2000 Mechanical stability of single DNA molecules *Biophys. J.* **78** 1997–2007
[234] Krautbauer R, Rief M and Gaub H E 2003 Unzipping DNA oligomers *Nano Lett.* **3** 493–6
[235] Schotanus M P, Aumann K S and Sinniah K 2002 Using force spectroscopy to investigate the binding of complementary DNA in the presence of intercalating agents *Langmuir* **18** 5333–6
[236] Osada T, Itoh A and Ikai A 2003 Mapping of the receptor-associated protein (RAP) binding proteins on living fibroblast cells using an atomic force microscope *Ultramicroscopy* **97** 353–7
[237] Horton M, Charras G and Lehenkari P 2002 Analysis of ligand–receptor interactions in cells by atomic force microscopy *J. Recept. Signal Transduct. Res.* **22** 169–90
[238] Chen A and Moy V T 2000 Cross-linking of cell surface receptors enhances cooperativity of molecular adhesion *Biophys. J.* **78** 2814–20
[239] Rief M, Oesterhelt F, Hetmann B and Gaub H E 1997 Single molecule force spectroscopy on polysaccharides by atomic force microscopy *Science* **276** 1295–7
[240] Rief M, Gautel M, Oesterhelt F, Fernandez J M and Gaub H E 1997 Reversible unfolding of individual titin immunoglobulin domains by AFM *Science* **276** 1109–12
[241] Janshoff A, Neitzert M, Oberdörfer Y and Fuchs H 2000 Force spectroscopy of molecular systems—single molecule spectroscopy of polymers and biomolecules *Angew. Chem. Int. Ed.* **39** 3212–37
[242] Bustamante C, Marko J F, Siggia E D and Smith S 1994 Entropic elasticity of lambda-phage DNA *Science* **265** 1599–600
[243] Odijk T 1995 Stiff chains and filaments under tension *Macromolecules* **28** 7016–8
[244] Bustamante C, Marko J F, Siggia E D and Smith S 1994 Entropic elasticity of lamba-phage DNA *Science* **265** 1599–600
[245] Marko J F and Siggia E D 1995 Stretching DNA *Macromolecules* **28** 8759–70
[246] Bustamante C, Smith S B, Liphardt J and Smith D 2000 Single-molecule studies of DNA mechanics *Curr. Opin. Struct. Biol.* **10** 279–85
[247] Krautbauer R, Pope L H, Schrader T E, Allen S and Gaub H E 2002 Discriminating small molecule binding modes by single molecule force spectroscopy *FEBS Lett.* **510** 154–8
[248] Bouchiat C, Wang M D, Allemand J F, Strick T, Block S M and Croquette V 1999 Estimating the persistence length of a worm-like chain molecule from force–extension measurements *Biophys. J.* **76** 409–13
[249] Cluzel P, Lebrun A, Heller C, Lavery R, Viovy J L, Chatenay D and Caron F 1996 DNA: an extensible molecule *Science* **271** 792–4
[250] Rief M, Clausen-Schaumann H and Gaub H E 1999 Sequence-dependent mechanics of single DNA molecules *Nat. Struct. Biol.* **6** 346–9
[251] Williams M C and Rouzina I 2002 Force spectroscopy of single DNA and RNA molecules *Curr. Opin. Struct. Biol.* **12** 330–6
[252] Smith S B, Cui Y and Bustamante C 1996 Overstretching B-DNA: the elastic response of individual double-stranded

and single-stranded DNA molecules *Science* **271** 795–9
[253] Rouzina I and Bloomfield V A 2001 Force-induced melting of the DNA double helix: 1. Themodynamic analysis *Biophys. J.* **80** 882–93
[254] Rouzina I and Bloomfield V A 2001 Force-induced melting of the DNA double helix: 2. Effect of solution conditions *Biophys. J.* **80** 894–900
[255] Smith S B, Cui Y and Bustamante C 1996 Overstretching B-DNA: the elastic response of individual double-stranded and single-stranded DNA molecules *Science* **271** 795–9
[256] Bonin M, Zhu R, Klaue Y, Oberstrass J, Oesterschulze E and Nellen W 2002 Analysis of RNA flexibility by scanning force spectroscopy *Nucleic Acids Res.* **30** e81
[257] Fisher T, Oberhauser A F, Carrion-Vasquez M, Marszalek P E and Fernandez J M 1999 The study of protein mechanics with the atomic force microscope *Trends Biochem. Sci.* **24** 379–84
[258] Fisher T E, Marszalek P E, Oberhauser A F, Carrion-Vazquez M and Fernandez J M 1999 The micro-mechanics of single molecules studied with atomic force microscopy *J. Physiol.* **520** 5–14
[259] Carrion-Vazquez M, Oberhauser A F, Fisher T E, Marszalek P E, Li H and Fernandez J M 2000 The mechanical topology of protein studied by AFM *Prog. Biophys. Mol. Biol.* **74** 63–91
[260] Carrion-Vazquez M, Oberhauser A F, Fowler S B, Marszalek P E, Broedel S E, Clarke J and Fernandez J M 1999 Mechanical and chemical unfolding of a single protein: a comparison *Proc. Natl Acad. Sci. USA* **96** 3694–9
[261] Oberhauser A F, Marszalek P E, Erickson H P and Fernandez J M 1998 The molecular elasticity of the extracellular matrix protein tenascin *Nature* **393** 181–5
[262] Rief M, Pascual J, Saraste M and Gaub H E 1999 Single molecule force spectroscopy of spectrin repeats: low unfolding forces in helix bundles *J. Mol. Biol.* **286** 553–61
[263] Li H, Oberhauser A F, Fowler S B, Clarke J and Fernandez J M 2000 Atomic force microscopy reveals the mechanical design of a modular protein *Proc. Natl Acad. Sci. USA* **97** 6527–31
[264] Li H B, Carrion-Vazquez M, Oberhauser A F, Marszalek P E and Fernandez J M 2000 Point mutations alter the mechanical stability of immunoglobulin modules *Nat. Struct. Biol.* **7** 1117–20
[265] Marszalek P E, Lu H, Li H B, Carrion-Vazquez M, Oberhauser A F, Schulten K and Fernandez J M 1999 Mechanical unfolding intermediates in titin modules *Nature* **402** 100–3
[266] Carl P, Kwok C H, Manderson G, Speicher D W and Discher D E 2001 Forced unfolding modulated by disulfide bonds in the Ig domains of a cell adhesion molecule *Proc. Natl Acad. Sci. USA* **98** 1565–70
[267] Müller D J, Baumeister W and Engel A 1999 Controlled unzipping of a bacterial surface layer with atomic force microscopy *Proc. Natl Acad. Sci. USA* **96** 13170–4
[268] Müller D J, Kessler M, Oesterhelt F, Moller C, Oesterhelt D and Gaub H E 2002 Stability of bacteriorhodopsin—helices and loops analyzed by single-molecule force spectroscopy *Biophys. J.* **83** 3578–88
[269] Oberhauser A F, Hansma P K, Carrion-Vazquez M and Fernandez J M 2001 Stepwise unfolding of titin under force-clamp atomic force microscopy *Proc. Natl Acd. Sci. USA* **98** 468–72
[270] Fernandez J M and Li H B 2004 Force-clamp spectroscopy monitors the folding trajectory of a single protein *Science* **303** 1674–8
[271] Schar-Zammaretti P, Ziegler U, Forster I, Groscurth P and Spichiger-Keller U E 2002 Potassium-selective atomic force microscopy on ion-releasing substrates and living cells *Anal. Chem.* **74** 4269–74
[272] Zammaretti P, Fakler A, Zaugg F and Spichiger-Keller U E 2000 Atomic force microscope: a tool for studying ionophores *Anal. Chem.* **72** 3689–95
[273] Butt H J, Siedle P, Seifert K, Fendler K, Seeger T, Bamberg E, Weisenhorn A L, Goldie K and Engel A 1993 Scan speed limit in atomic force microscopy *J. Microsc.* **169** 75–84
[274] Walters D A, Cleveland J P, Thomson N H, Hansma P K, Wendman M A, Gurley G and Elings V 1996 Short cantilevers for atomic force microscopy *Rev. Sci. Instrum.* **67** 3583–90
[275] Ando T, Kodera N, Takai E, Maruyama D, Saito K and Toda A 2001 A high-speed atomic force microscope for studying biological macromolecules *Proc. Natl Acad. Sci. USA* **98** 12468–72
[276] Mamin H J, Birk H, Wimmer P and Rugar D 1994 High-speed scanning-tunneling-microscopy—principles and applications *J. Appl. Phys.* **75** 161–8
[277] Sulchek T, Yaralioglu G G, Quate C F and Minne S C 2002 Characterization and optimisation of scan speed for tapping-mode atomic force microscopy *Rev. Sci. Instrum.* **73** 2928–36
[278] Sulchek T, Hsieh R, Adams J D, Yaralioglu G G, Minne S C, Quate C F, Cleveland J P, Atalar A and Adderton D M 2000 High-speed tapping mode imaging with active Q control for atomic force microscopy *Appl. Phys. Lett.* **76** 1473–5
[279] Viani M B, Schäfer T E, Chand A, Rief M, Gaub H E and Hansma P K 1999 Small cantilevers for force spectroscopy of single molecules *J. Appl. Phys.* **86** 2258–62
[280] Viani M B *et al* 1999 Fast imaging and fast force spectroscopy of single biopolymers with a new atomic force microscope designed for small cantilevers *Rev. Sci. Instrum.* **70** 4300–3
[281] Minne S C, Yaralioglu G, Manalis S R, Adams J D, Zesch J, Atalar A and Quate C F 1998 Automated parallel high-speed atomic force microscopy *Appl. Phys. Lett.* **72** 2340–2
[282] Proksch R, Lal R, Hansma P K, Morse D and Stucky G 1996 Imaging the internal and external pore structure of membranes in fluid: tapping mode scanning ion conductance microscopy *Biophys. J.* **71** 2155–7
[283] Gardner C E and Macpherson J V 2002 Atomic force microscopy probes go electrochemical *Anal. Chem.* **74** 576A–84A